technische universiteit eindhoven

Geometric Models of the Visual Front-End

Bart ter Haar Romeny

Eindhoven University of Technology
Biomedical Image Anaysis & Interpretation
Eindhoven, the Netherlands

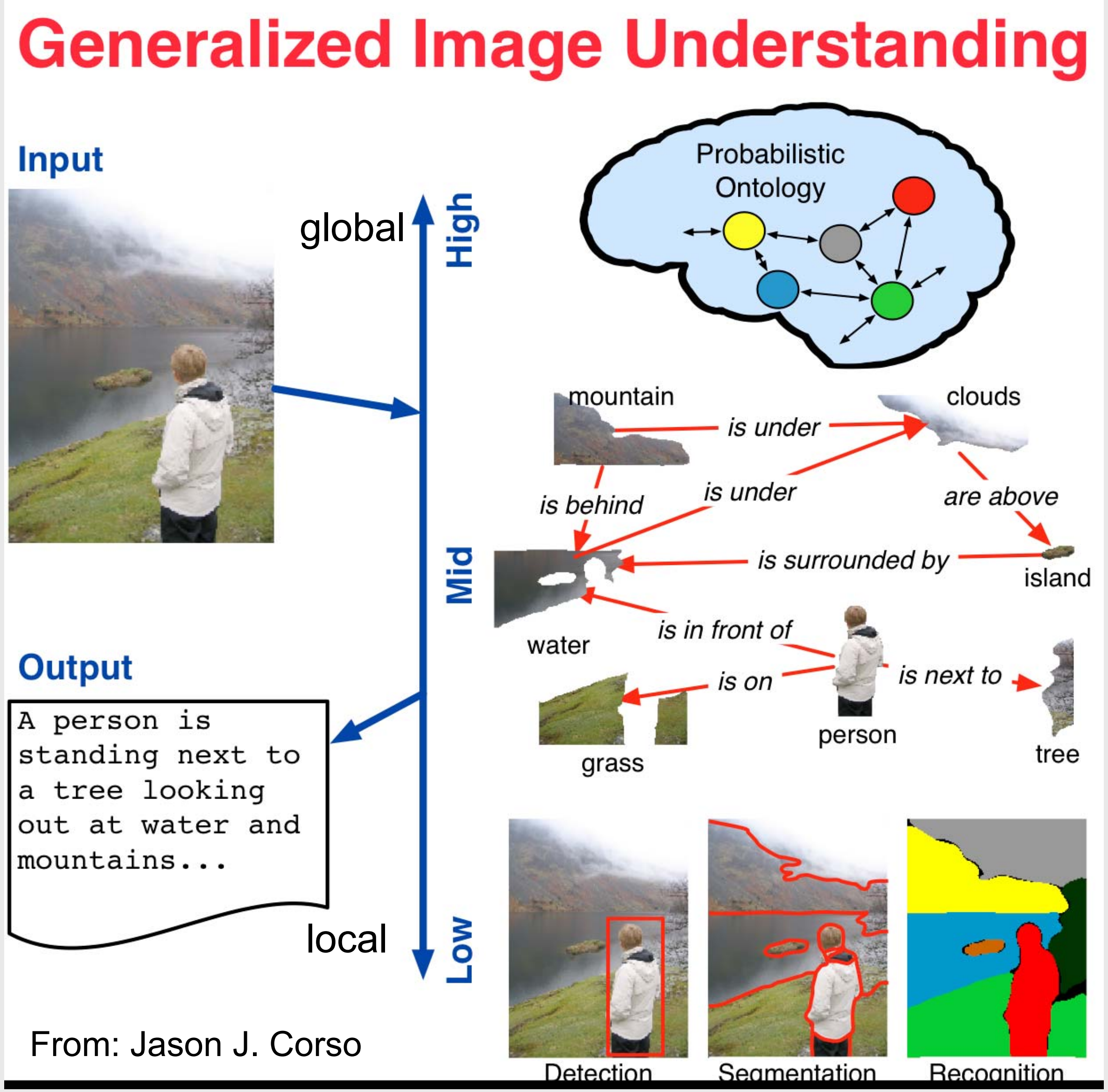

From: Jason J. Corso

Geometric models
task = geometry inference
Self-organization:
– axioms, mathematics

Pattern recognition
– S-COSFIRE contextual model
Self-organization:
– learning, Hebbian rules, neural nets

This talk: **early vision geometry.**

How can we explain the extremely well organized very extensive filter banks?

→ HPC,
Computer-Aided Diagnosis

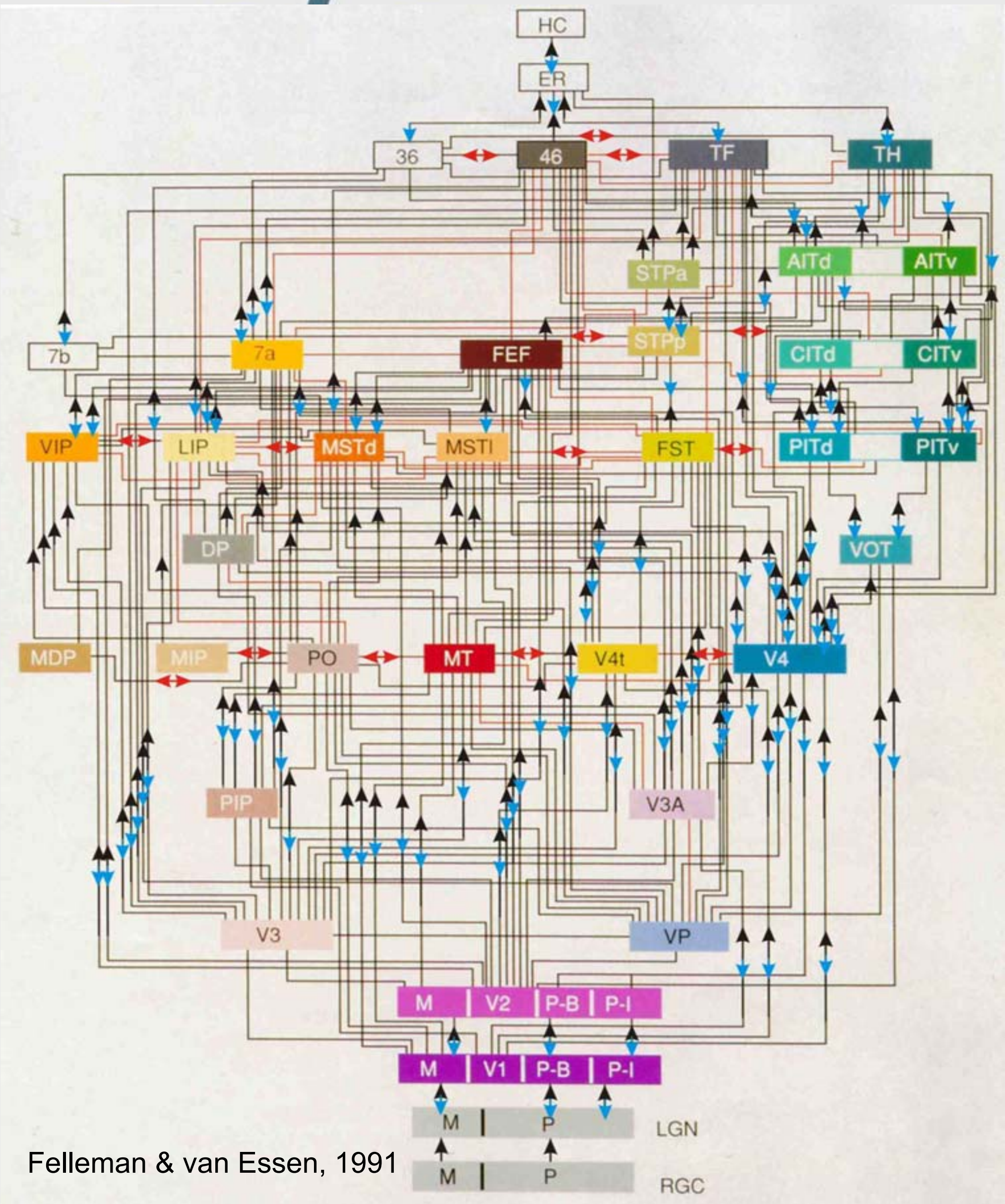

Felleman & van Essen, 1991

Vision is the most extensively studied function in the brain.

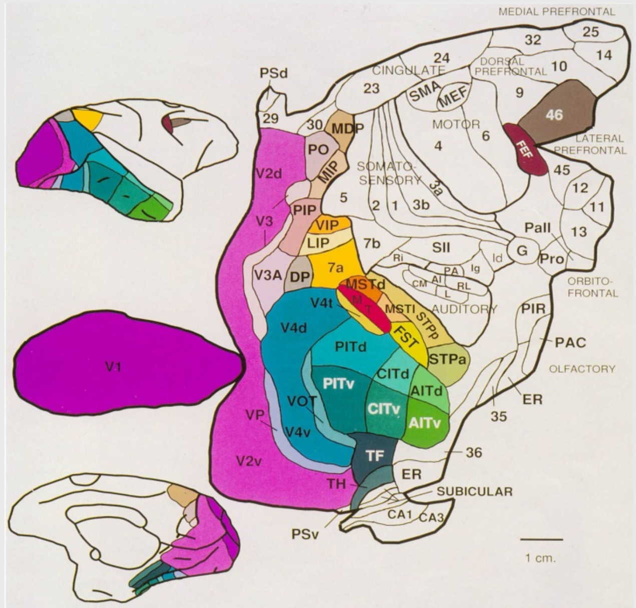

Multi-scale sampling at the retina:
measuring at many resolutions simultaneously

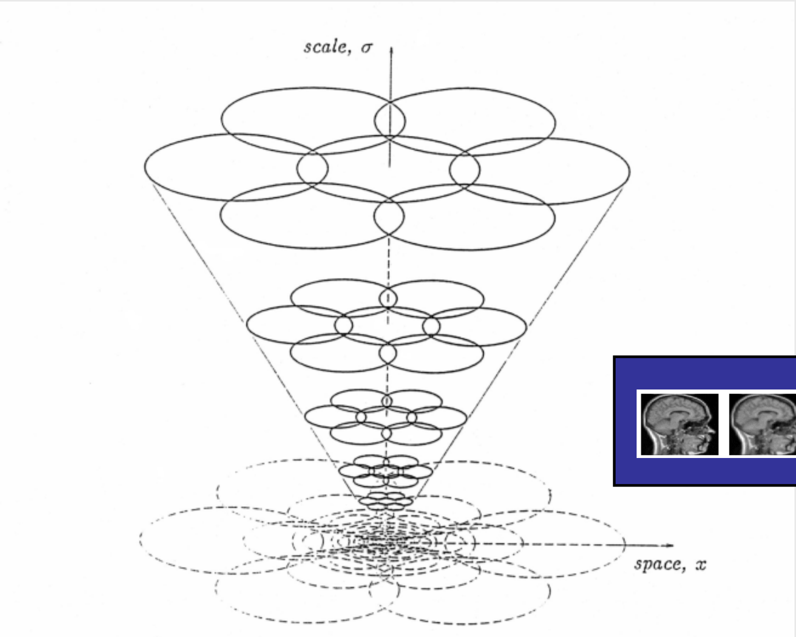

Retinal stack model
(Lindeberg 1994,
Koenderink 1990)

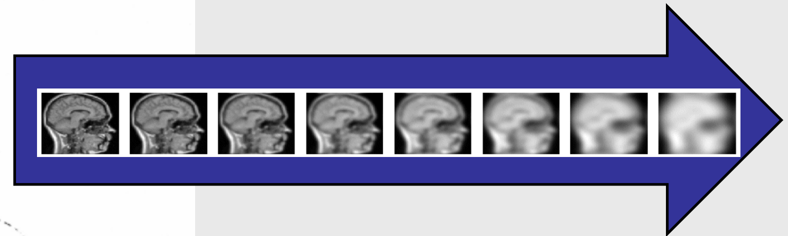

Deep structure

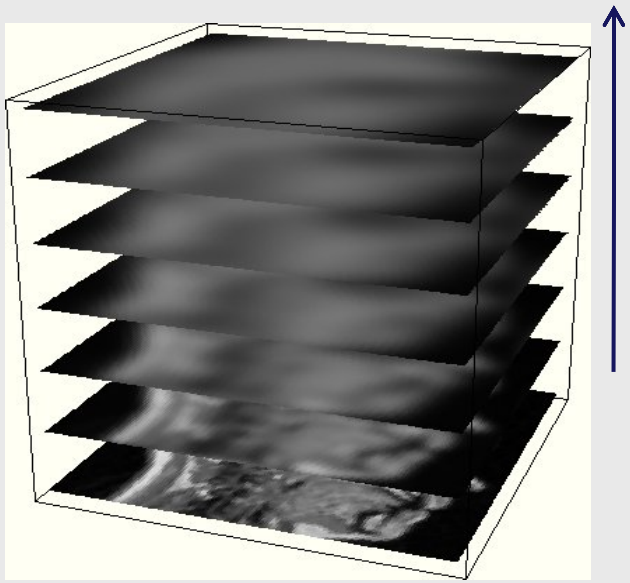

scale-space

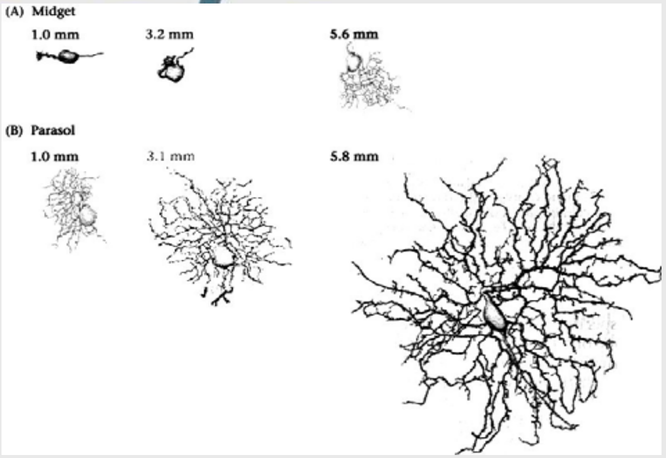

Receptive
field
mapping

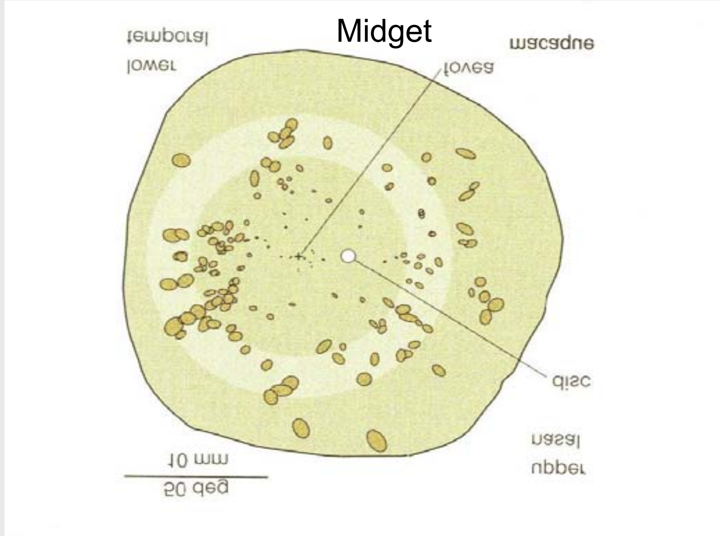

Two types of retinal ganglion cells:
Parasol: large, for motion
Midget: small, for shape

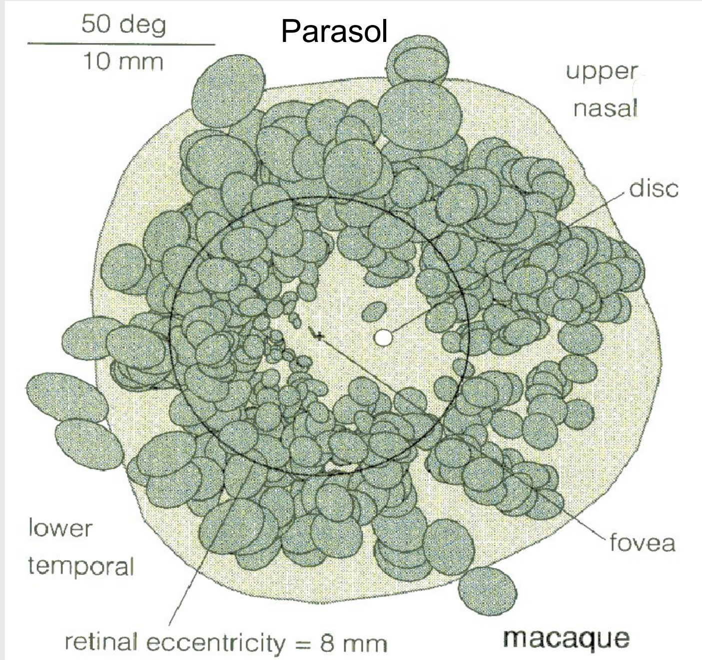

On-center
Off-center

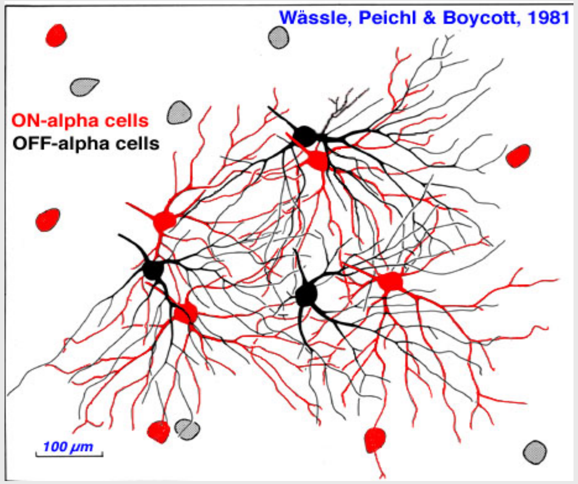

Rodieck 2004 : ‘The first steps of seeing’

Multi-scale retina:
measuring at many resolutions simultaneously

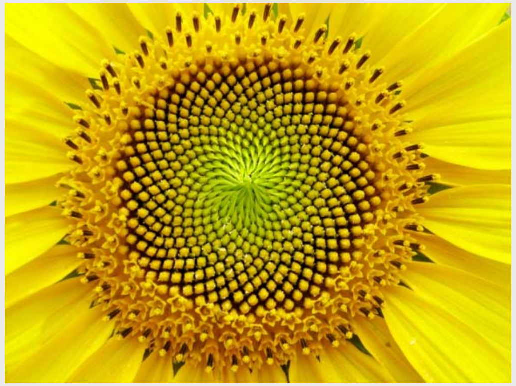

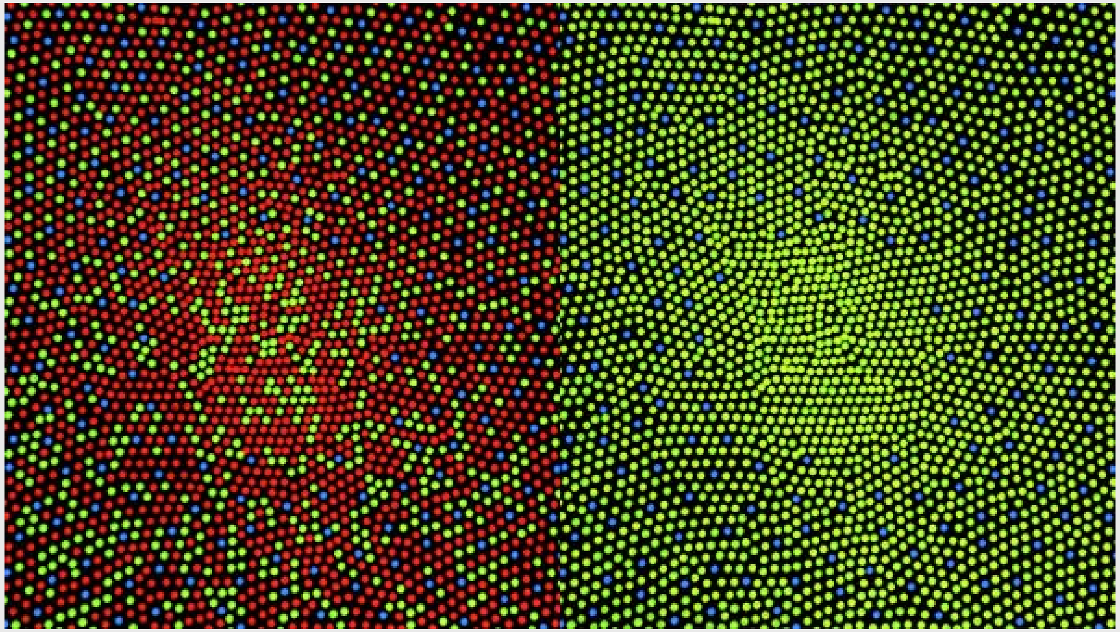

Human foveal receptors

Color blind

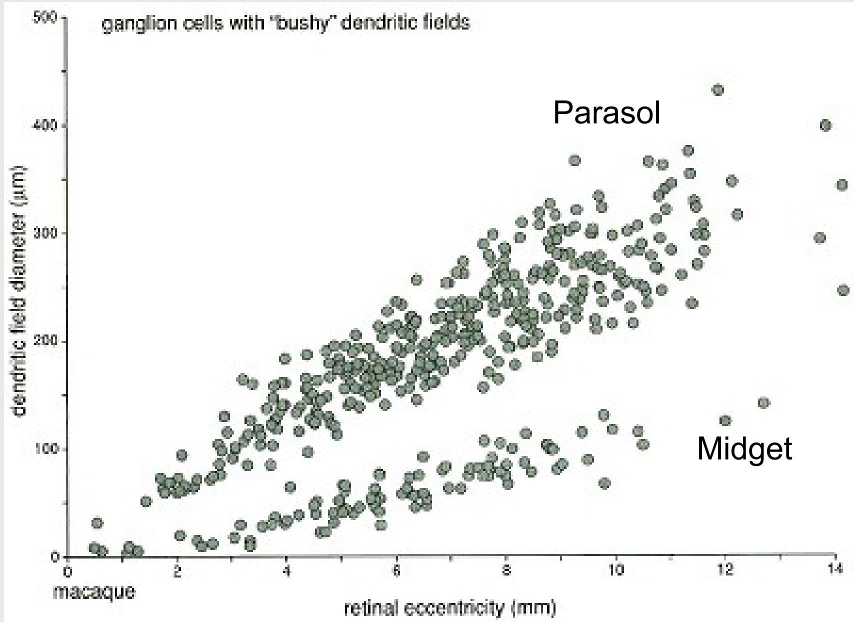

Rodieck, 2004

'Spurious resolution': artefact of the wrong aperture (Koenderink, 1990)

First principles derivation of the Gaussian kernel as optimal aperture

A. The aperture function $g(x)$ should be a *normalized* filter:

$$\int_{-\infty}^{\infty} g(x)\, dx = 1.$$

B. The *mean* of the filter $g(x)$ is

$$\int_{-\infty}^{\infty} x\, g(x)\, dx = x_0 = 0.$$

C. The *width* is the variance:

$$\int_{-\infty}^{\infty} x^2\, g(x)\, dx = \sigma^2.$$

Minimal entropy of our filter:

$$H = \int_{-\infty}^{\infty} -g(x) \ln g(x)\, dx.$$

<u>Unique</u> solution:

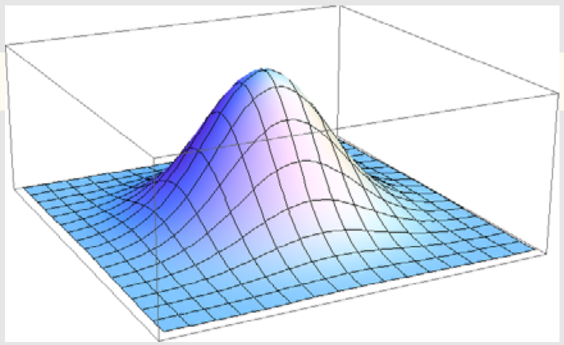

Gaussian kernel

The energy *E* becomes:

$$E = -\int_{-\infty}^{\infty} g(x) \ln g(x)\, dx + \lambda_1 \int_{-\infty}^{\infty} g(x)\, dx + \lambda_2 \int_{-\infty}^{\infty} x\, g(x)\, dx + \lambda_3 \int_{-\infty}^{\infty} x^2 g(x)\, dx$$

and is minimum when $\frac{\delta E}{\delta g} = 0$. The λ's are the *Lagrange multipliers* .

```
Clear[g];
<< VariationalMethods`;
var = VariationalD[-g[x] Log[g[x]] + λ1 g[x] + λ2 x g[x] + λ3 x^2 g[x], g[x], x]
```

```
-1 + λ1 + x λ2 + x^2 λ3 - Log[g[x]]
```

```
g[x_] = First[g[x] /. Solve[var == 0, g[x]]]
```

$e^{-1+\lambda_1+x\lambda_2+x^2\lambda_3}$

An important first finding is that *g* is an exponential function.

```
eqn1 @ Simplify⌊⌊ ¯ g⌊x⌊ žx @@ 1, ○3 ? 0⌊
               0—
```

```
Ÿ √0 ○3  fl  Ÿ^(○1 0 (○2 2)/(4 ○3))  √s
```

```
eqn2 @ Simplify⌊⌊ ¯ x g⌊x⌊ žx fl 0, ○3 ? 0⌊
               0—
```

```
Ÿ^(○1 0 (○2 2)/(4 ○3))  ○2 fl 0
```

```
eqn3 @ Simplify⌊⌊ ¯ x² g⌊x⌊ žx @@ v², ○3 ? 0⌊
               0—
```

```
Ÿ^(01 . ○1 0 (○2 2)/(4 ○3)) ⌊√s ⌊○2² 0 2 ○3⌊
───────────────────────────────────────────────  fl v²
           4 ⌊0 ○3⌊^5 ⌊²
```

technische universiteit eindhoven

Now we can solve for all three λ's:

```
solution = Solve[{eqn1, eqn2, eqn3}, {λ1, λ2, λ3}, Method -> "Legacy"]
```

$$\left\{\left\{\lambda_1 \to \frac{1}{4}\,\mathrm{Log}\left[\frac{e^4}{4\,\pi^2\,\sigma^4}\right],\ \lambda_2 \to 0,\ \lambda_3 \to -\frac{1}{2\,\sigma^2}\right\}\right\}$$

```
g[x_, σ_] = Simplify[g[x] /. Flatten[solution], σ > 0]
```

$$\frac{e^{-\frac{x^2}{2\,\sigma^2}}}{\sqrt{2\,\pi}\;\sigma}$$

which is the Gaussian function. A beautiful result. We have found the Gaussian as the *unique* solution to the set of constraints, which in principle are a formal statement of the *uncommittment* of the observation.

There are 11 known axiomatic derivations of the Gaussian kernel as the optimal aperture for uncommitted observations [Weickert 2002].

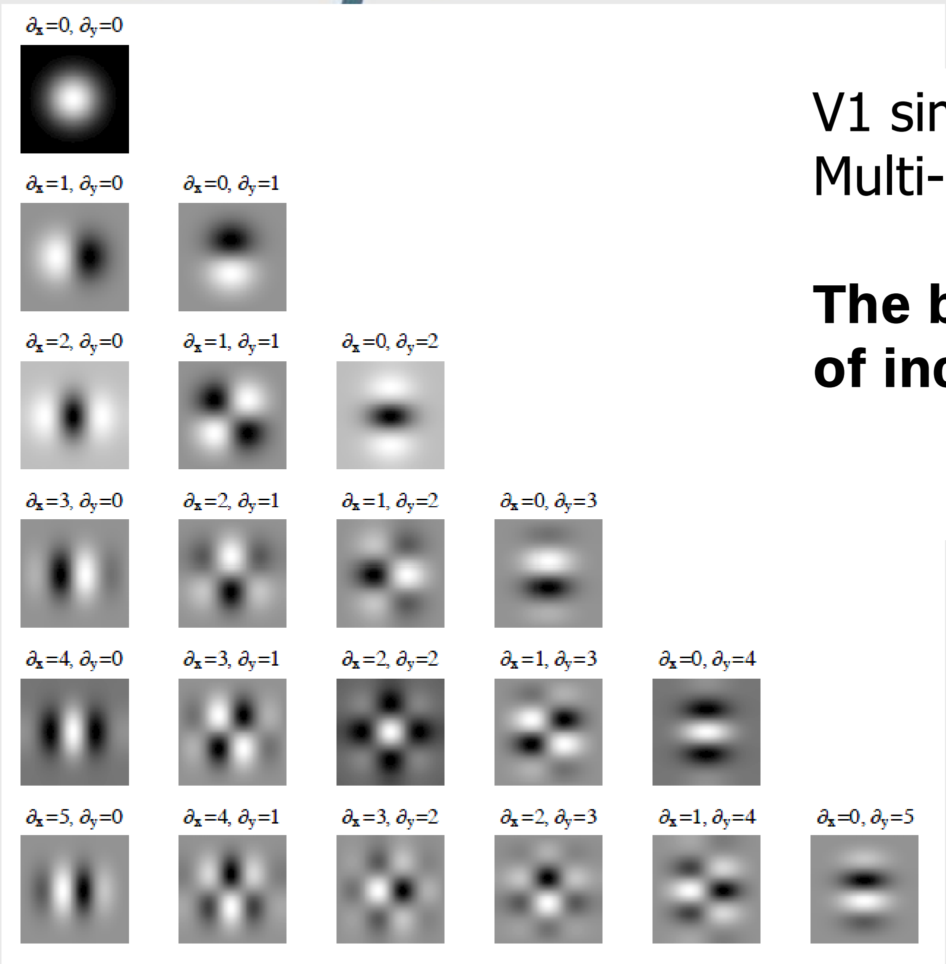

Gaussian derivatives to 5th order

V1 simple cells receptive fields model:
Multi-scale differential operators

The brains takes high order derivatives of incoming images, up to 4th order.

(Young 1991, Koenderink 1994)

$$\frac{\partial}{\partial x}\left\{L_0(\boldsymbol{x}) \otimes G(\boldsymbol{x};\sigma)\right\} = L_0(\boldsymbol{x}) \otimes \frac{\partial}{\partial x} G(\boldsymbol{x};\sigma)$$

High order differential geometry, features, shape …

Mathematica demo

Eigenpatches: PCA analysis

A PCA analysis of the patches:

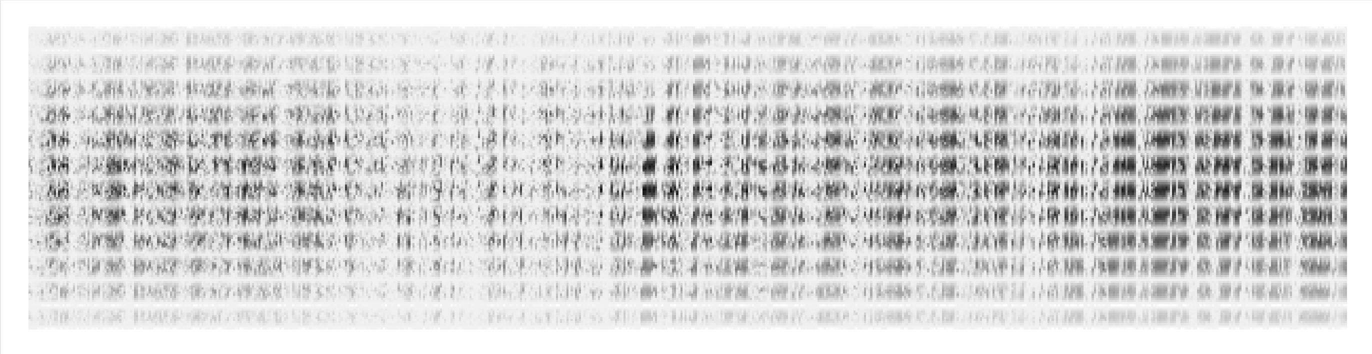

$m^T m$

$\longrightarrow$

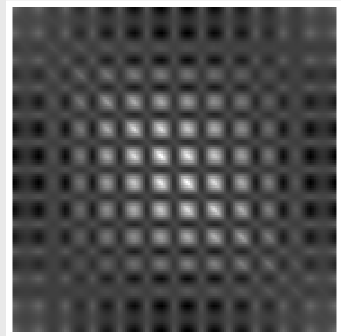

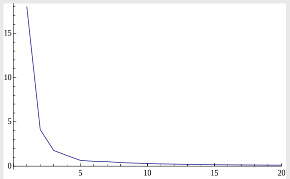

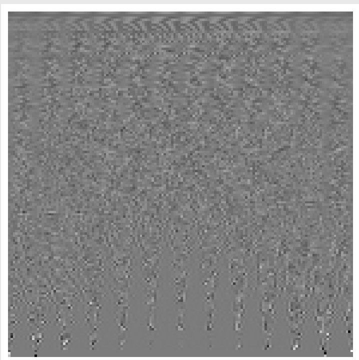

Partition

$\longrightarrow$

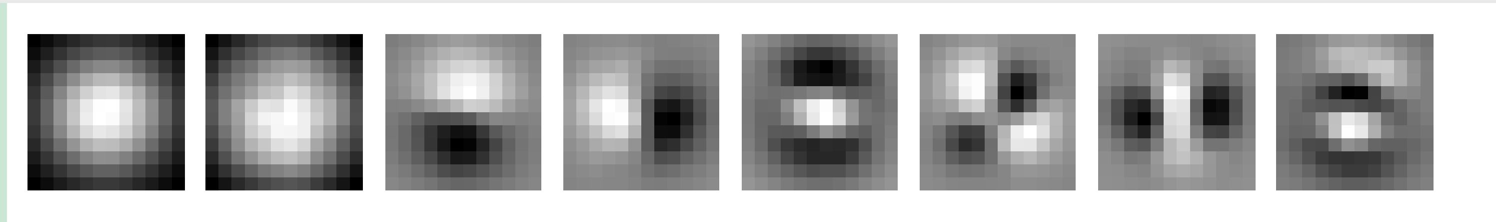

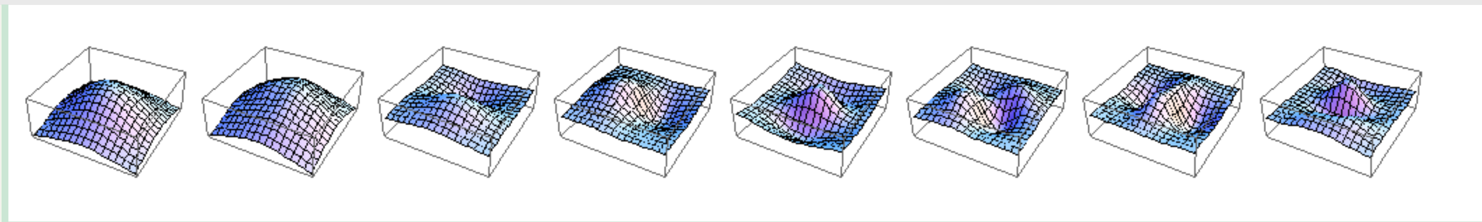

Movie:
cat trained with horizontal bars
(Colin Blakemore, Oxford)
3:30 6:06

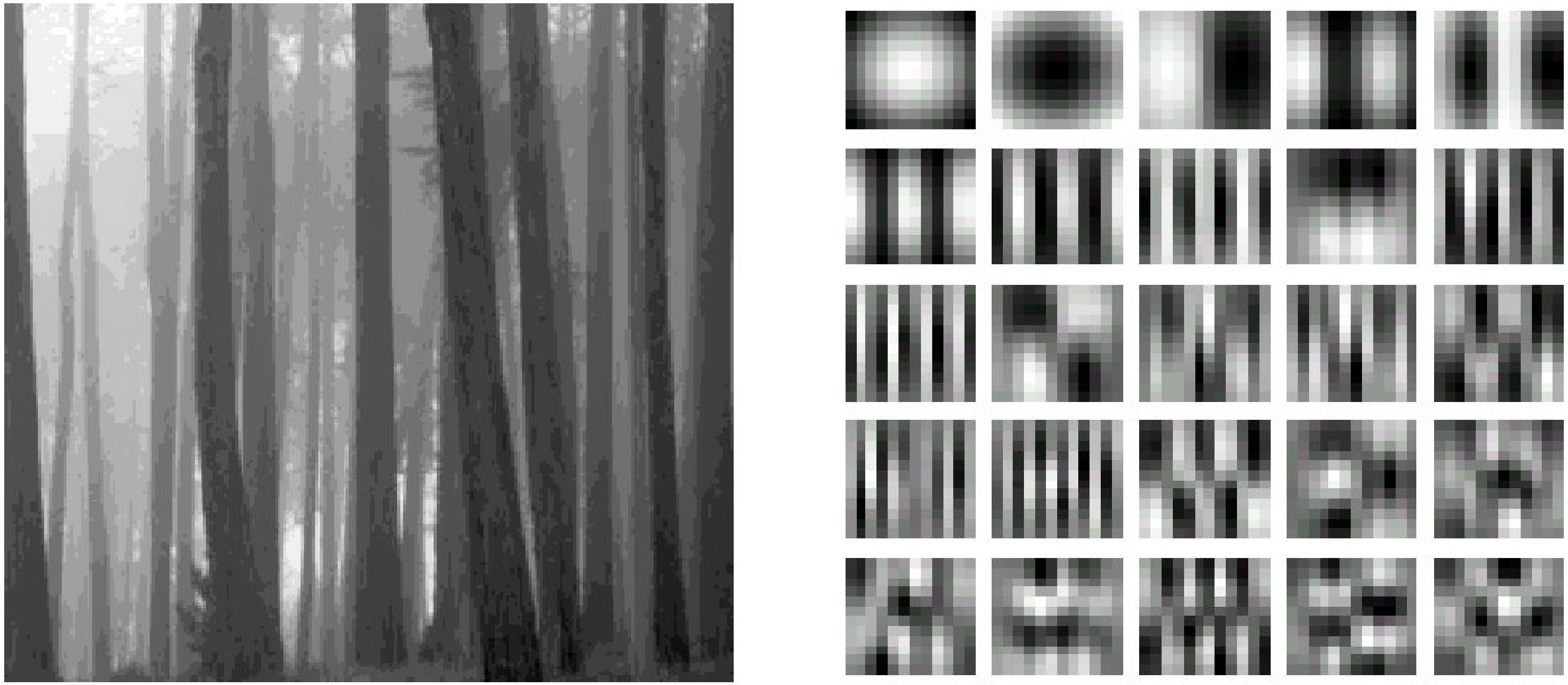

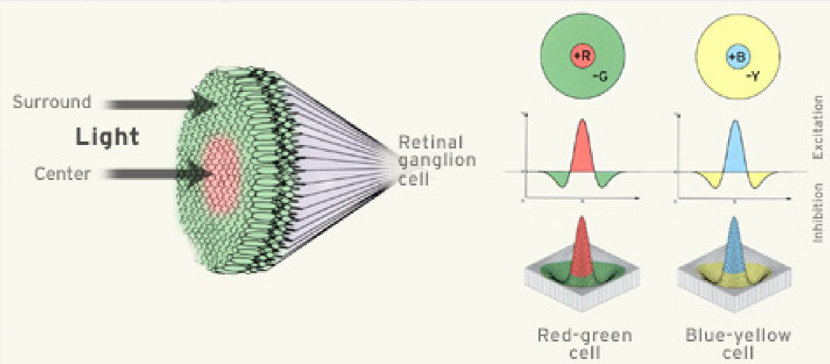

Retinal receptive fields have a center-surround structure.

50% on-center,
50% off-center

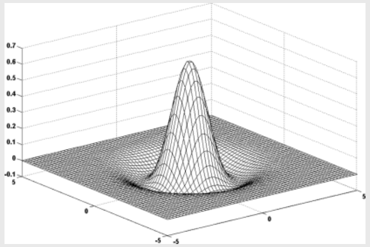

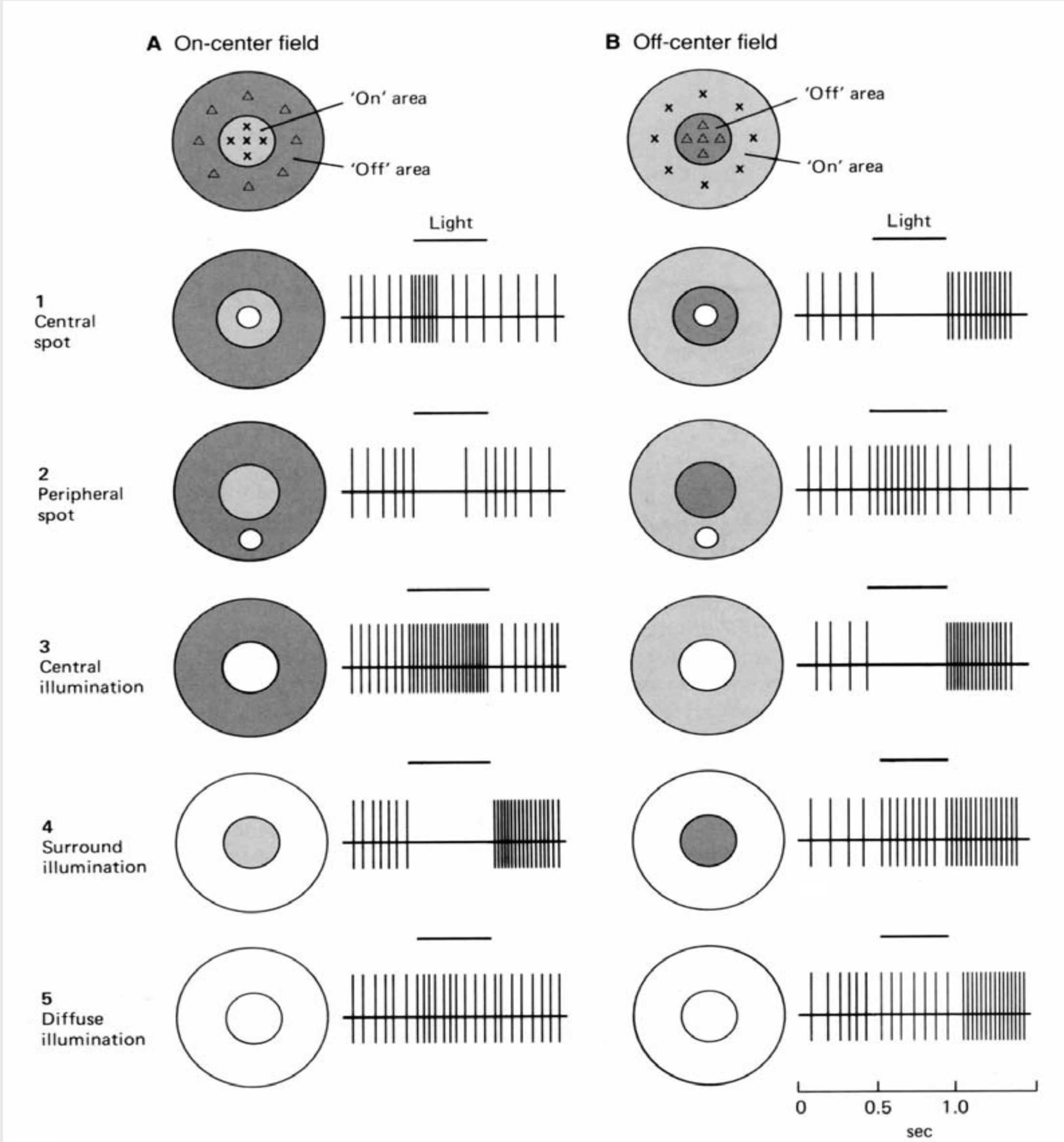

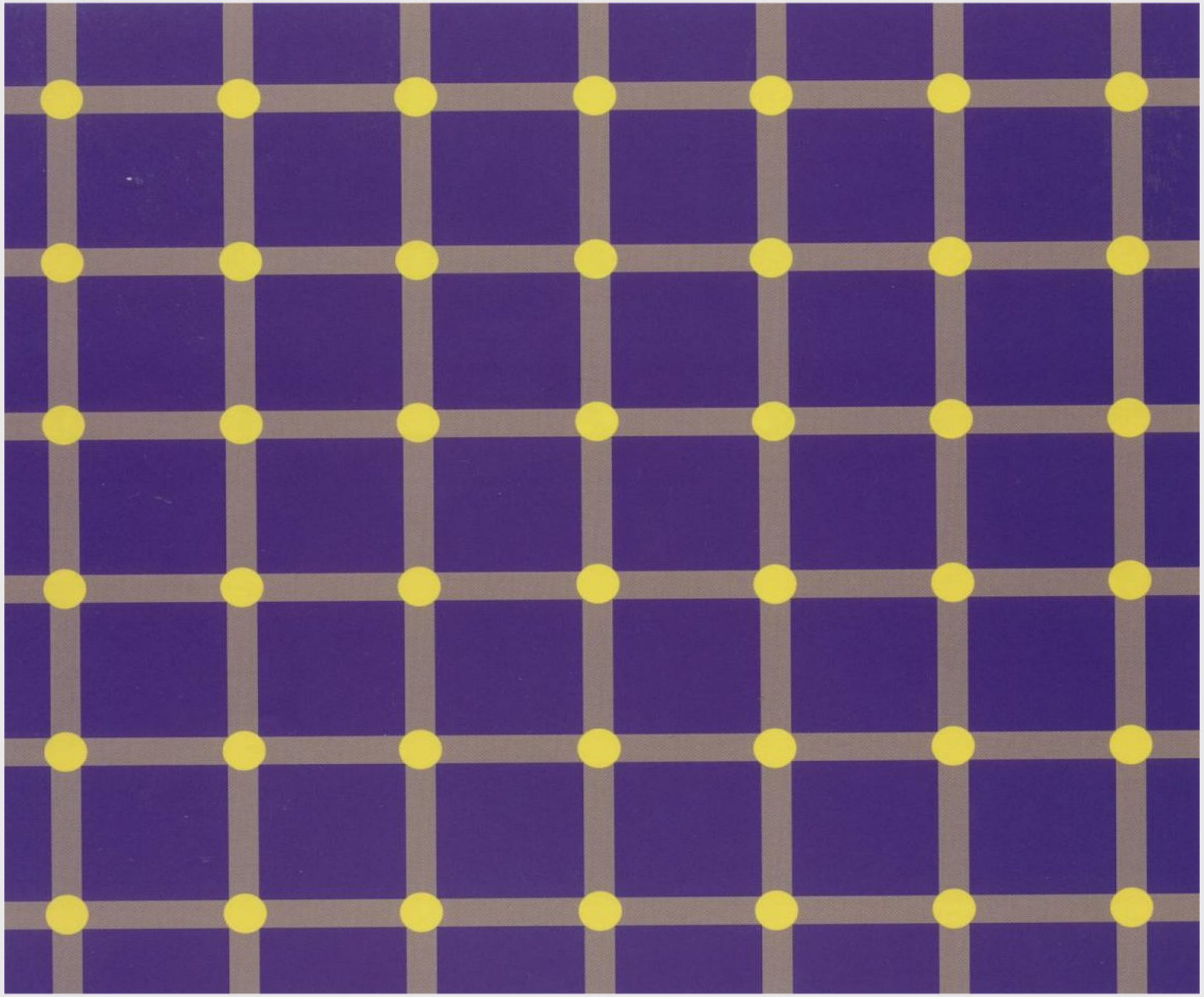

technische universiteit eindhoven

Koenderink: the Gaussian induces a multi-scale paradigm.
scale is free parameter.

The Gaussian is the Green's function of the diffusion equation:

$$\frac{\partial L}{\partial s} = \frac{\partial^2 L}{\partial x^2} + \frac{\partial^2 L}{\partial y^2}$$

Center-surround model: Laplacian of Gaussian kernel.

Why do we measure with a Laplacian? 'Lateral inhibition'.
We may measure only points of interest,
with change of RF size.

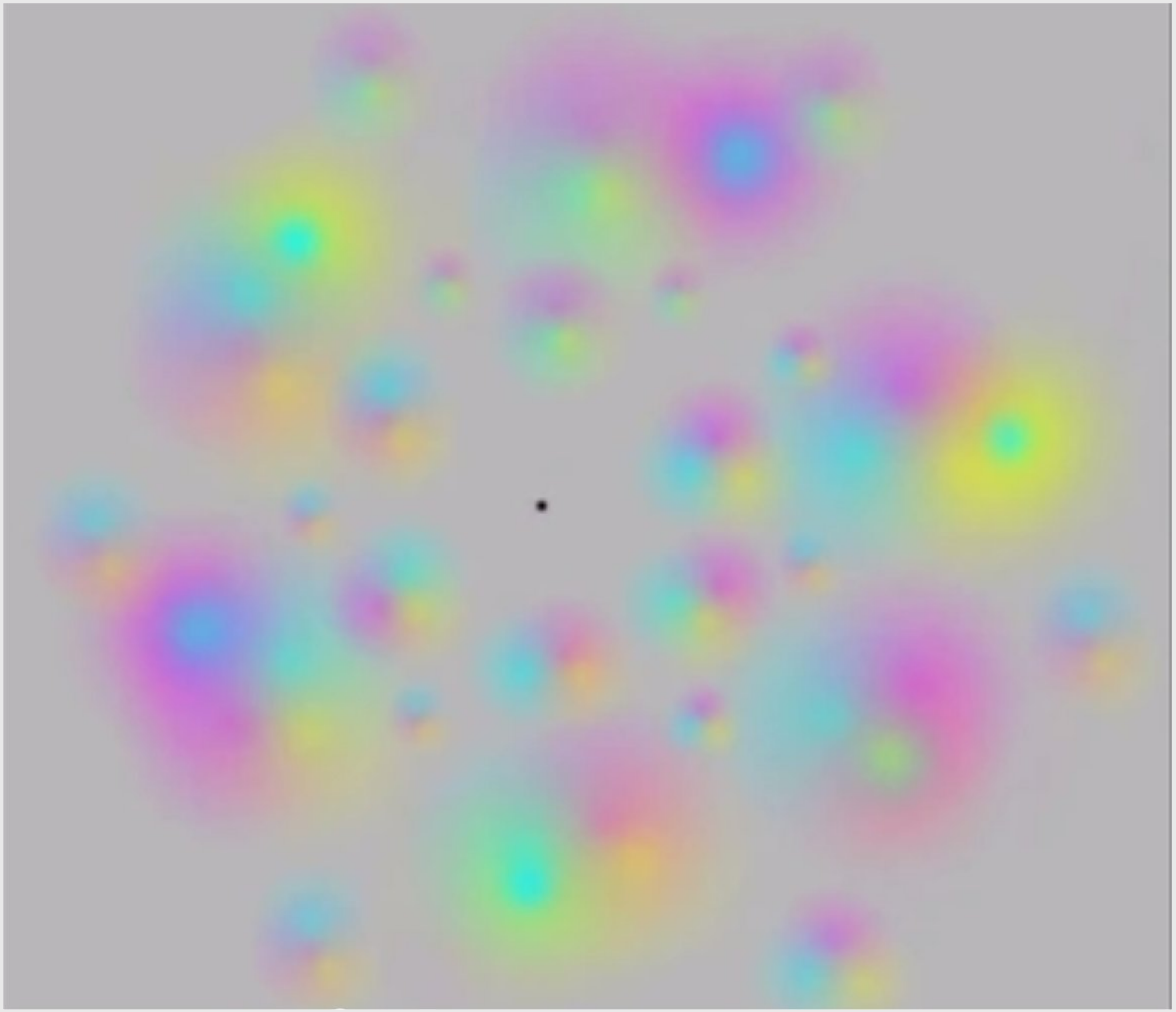

Troxler's fading:

With stabilized retinal images vision disappears.

Regularization:

- smoothing the data, convolution with some kernel;
- interpolation, by a polynomial (multidimensional) function;
- energy minimization, of a cost function under constraints
- fitting a function to the data (e.g. cubic splines);
- graduated convexity [Blake1987];
- deformable templates ('snakes') [McInerney1996];
- thin plates splines [Bookstein1989];
- Tikhonov regularization.

$T_L =$ + - ¥

$\P_{i_1 \ldots i_n} T_L =$ 1 - ¥ $\P_{i_1 \ldots i_n}$ f â x

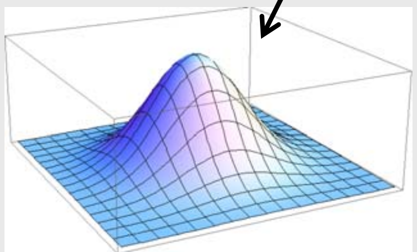

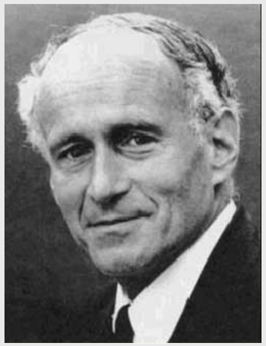

Uj~{nw}!\lq¢j{}¥
1:B:>ƅ;99<2!

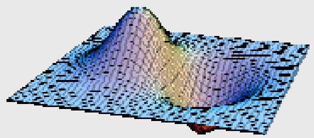

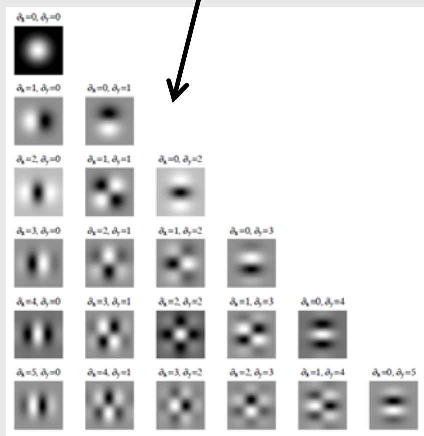

Mathematics	•	Smooth test function
Computer vision	•	Kernel, filter
Biological vision	•	Receptive field

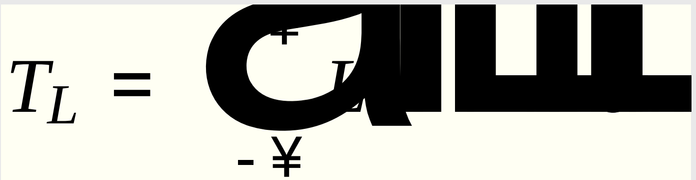

Schwartz 1959

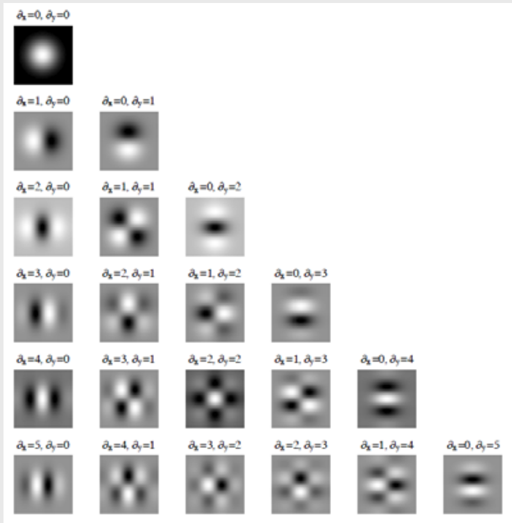

Koenderink 1994

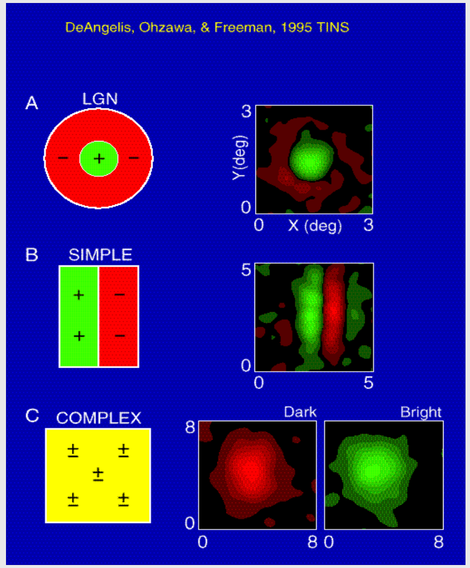

Ohzawa & Freeman 1995

technische universiteit eindhoven

Relation regularization - Gaussian scale-space

An essential result in scale-space theory was shown by Mads Nielsen (Copenhagen University). He proved that Tikhonov regularization is essentially equivalent to convolution with a Gaussian kernel.

$$E(g)=\int_{-\infty}^{\infty}(f-g)^2\,dx$$

minimize this function for g, given the constraint that the derivative behaves well.

Euler-Lagrange: $$E(g)=\int_{-\infty}^{\infty}\left((f-g)^2+\lambda g_x^2\right)dx$$

In the Fourier domain the expressions are easier:

$$E(g) = \mathcal{F}\left[\left(\tilde{f} - \tilde{g}\right)^2 + \lambda_1 g_x^2\right] = \int \left(\tilde{f} - \tilde{g}\right)^2 + \lambda_1 \tilde{g}_x^{\,2} = \int \left(\tilde{f} - \tilde{g}\right)^2 + \lambda_1 \omega^2 \tilde{g}^2$$

$$\frac{d E(\tilde{g})}{d \tilde{g}} = 2\left(\tilde{f} - \tilde{g}\right) + 2\lambda_1 \omega^2 \tilde{g} = 0$$

$$\left(\tilde{f} - \tilde{g}\right) + \lambda_1 \omega^2 \tilde{g} = 0 \Leftrightarrow \tilde{g} = \frac{1}{1+\lambda_1 \omega^2} \tilde{f}$$

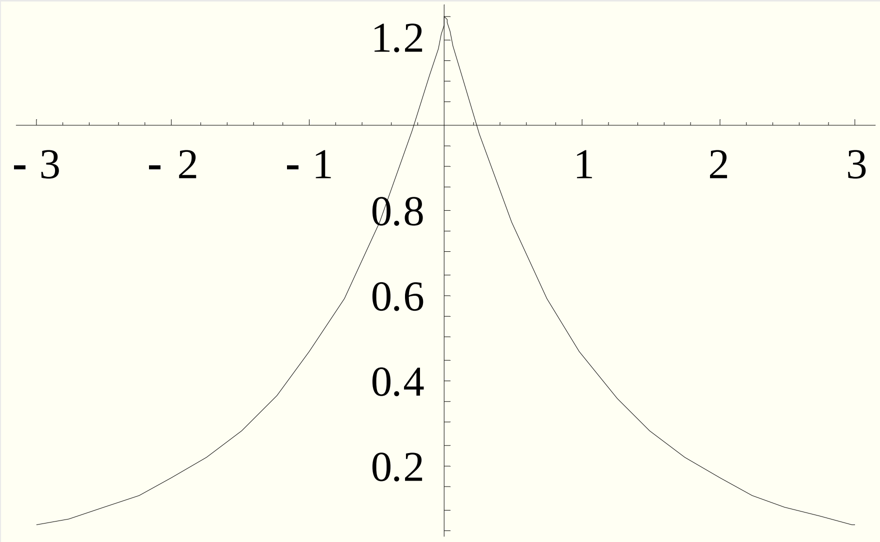

Filter proposed by Castan, 1990

In the spatial domain:

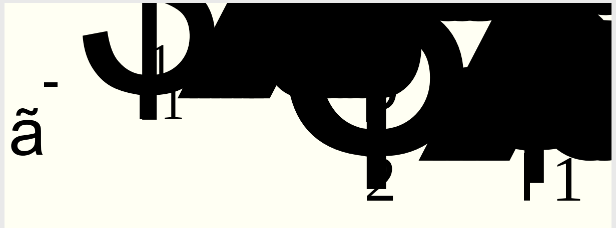

Including the second order derivative:

$$E(g) = \int \left[(\tilde{f} - g)^2 + \lambda_1 g_x^2 + \lambda_2 g_{xx}^2 \right] dx = \int_{-\infty}^{\infty} \left[(\tilde{f} - \tilde{g})^2 + \lambda_1 \omega^2 \tilde{g}^2 + \lambda_2 \omega^4 \tilde{g}^2 \right] d\omega$$

$$\frac{dE(g)}{dg} = 2(\tilde{f} - g) + 2\lambda_1 \omega^2 g + 2\lambda_2 \omega^4 g = 0$$

$$\tilde{g} = \frac{1}{1 + \lambda_1 \omega^2 + \lambda_2 \omega^4} \tilde{f}$$

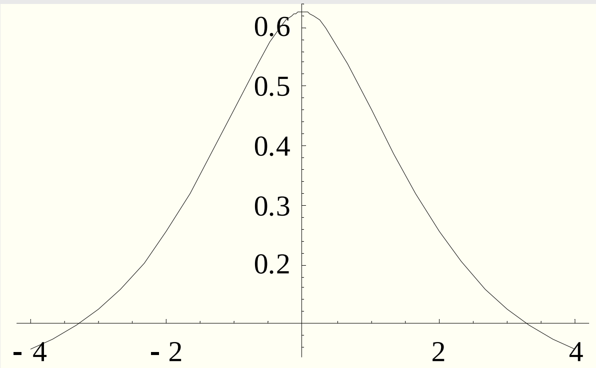

Function proposed by Deriche (1987)

etc.

Taylor expansion of the Gaussian in the Fourier domain:

$$\frac{e^{-\frac{1}{2}\sigma^2\omega^2}}{\sqrt{2\pi}} = 1 + \frac{\sigma^2\omega^2}{2} + \frac{\sigma^4\omega^4}{8} + \frac{\sigma^6\omega^6}{48} + \frac{\sigma^8\omega^8}{384} + \frac{\sigma^{10}\omega^{10}}{3840} + O(\omega^{11})$$

By recursion:

Tikhonov regularization
is equivalent to Gaussian blurring

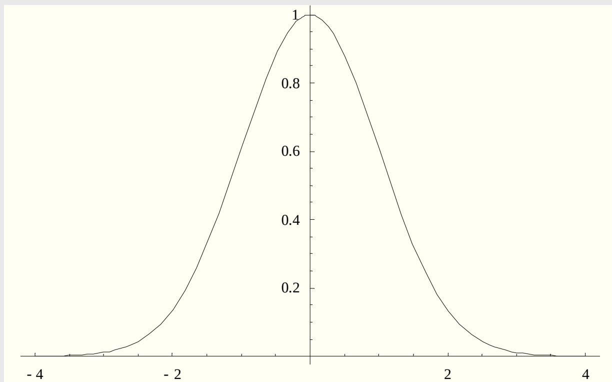

An example of high order derivatives and regularization:

Deblurring with a scale-space approach

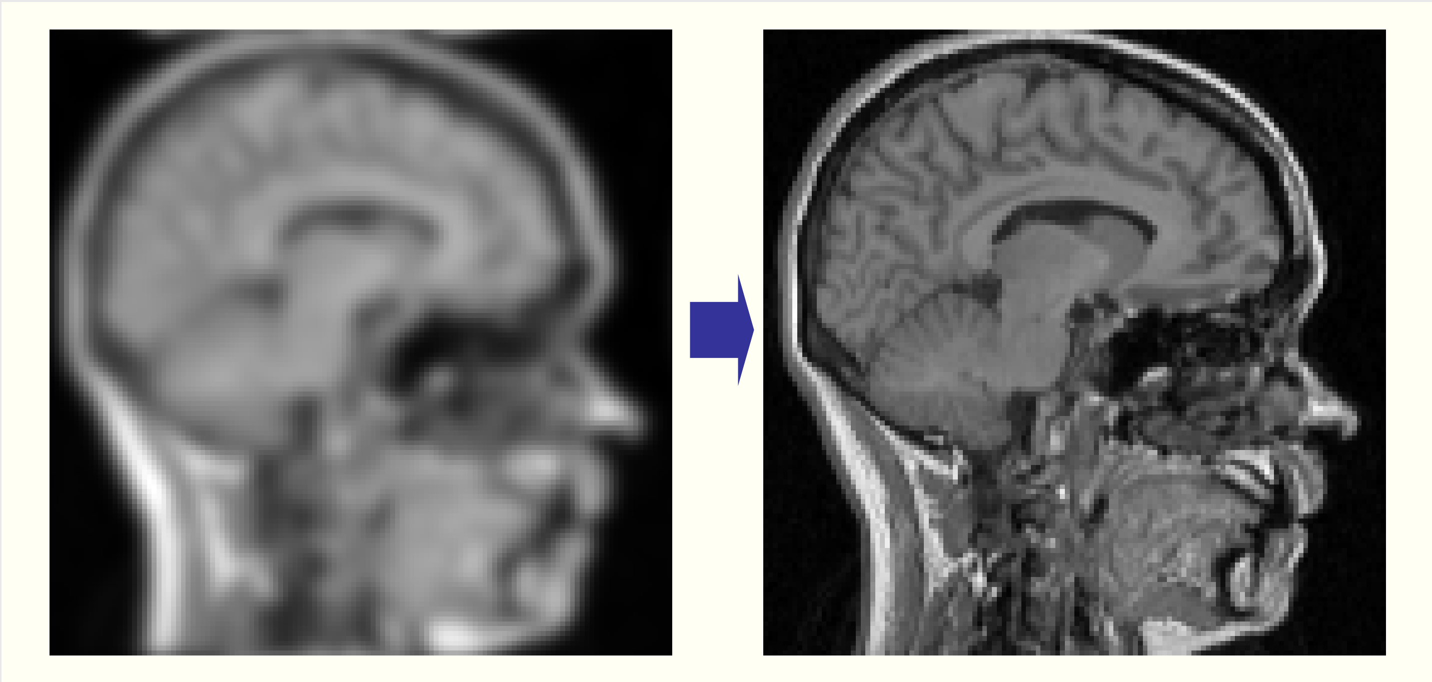

Can we inverse the diffusion equation?

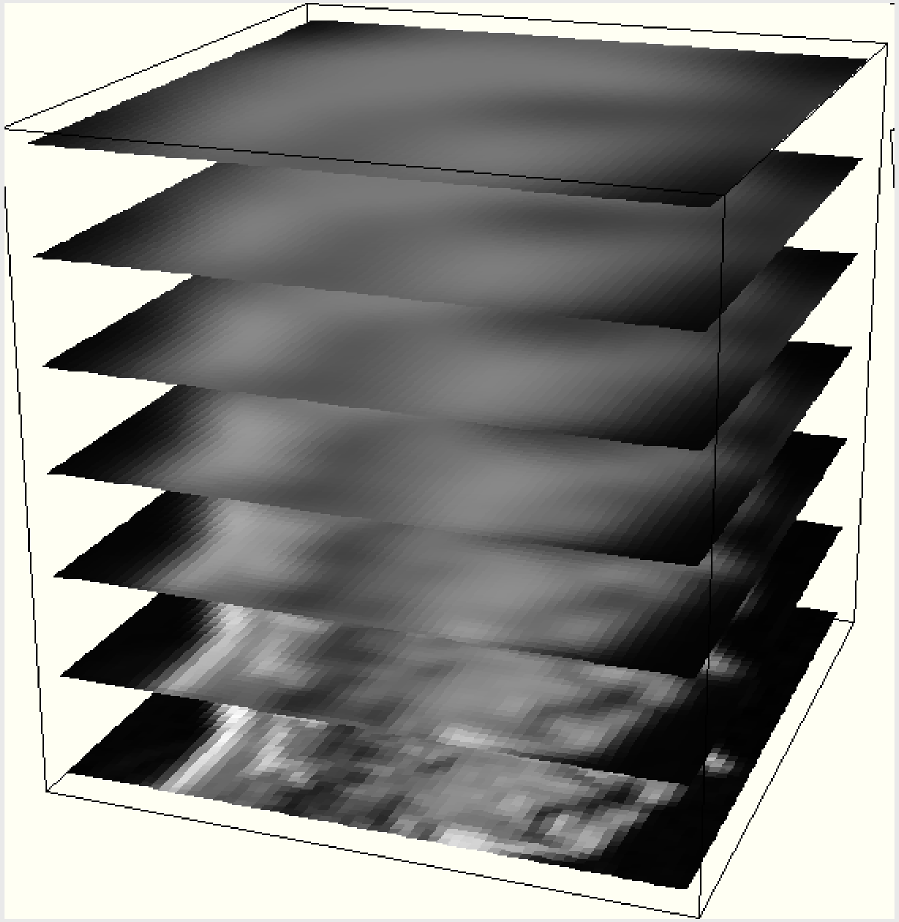

Recall that scale-space is infinitely differentiable due to the regularization properties of the observation process.

We can construct a Taylor expansion of the scale-space in any direction, including the negative scale direction.

Taylor expansion 'downwards':

$$L(x, y, s - \delta s) = L - \frac{\partial L}{\partial s}\delta s + \frac{1}{2!}\frac{\partial^2 L}{\partial s^2}\delta s^2 - \frac{1}{3!}\frac{\partial^3 L}{\partial s^3}\delta s^3 + O(\delta s^4)$$

The derivatives with respect to s (scale) can be expressed in spatial derivatives due to the diffusion equation

$$\frac{\partial L}{\partial s} = \frac{\partial^2 L}{\partial x^2} + \frac{\partial^2 L}{\partial y^2}$$

$$L(x, y, s - \delta s) = L - \delta s \left(\frac{\partial^2 L}{\partial x^2} + \frac{\partial^2 L}{\partial y^2} \right) + \frac{1}{2!} \delta s^2 \left(\frac{\partial^4 L}{\partial x^4} + 2 \frac{\partial^4 L}{\partial x^2 \partial L^2} + \frac{\partial^4 L}{\partial y^4} \right) + O(\delta s^3)$$

It is well-known that subtraction of the Laplacian sharpens the image. It is the first order approximation of the deblurring process.

technische universiteit eindhoven

Deblurring to 4^{th}, 8^{th}, 16^{th} and 32^{nd} order:

There are 560 derivative terms in the 32^{nd} order expression!

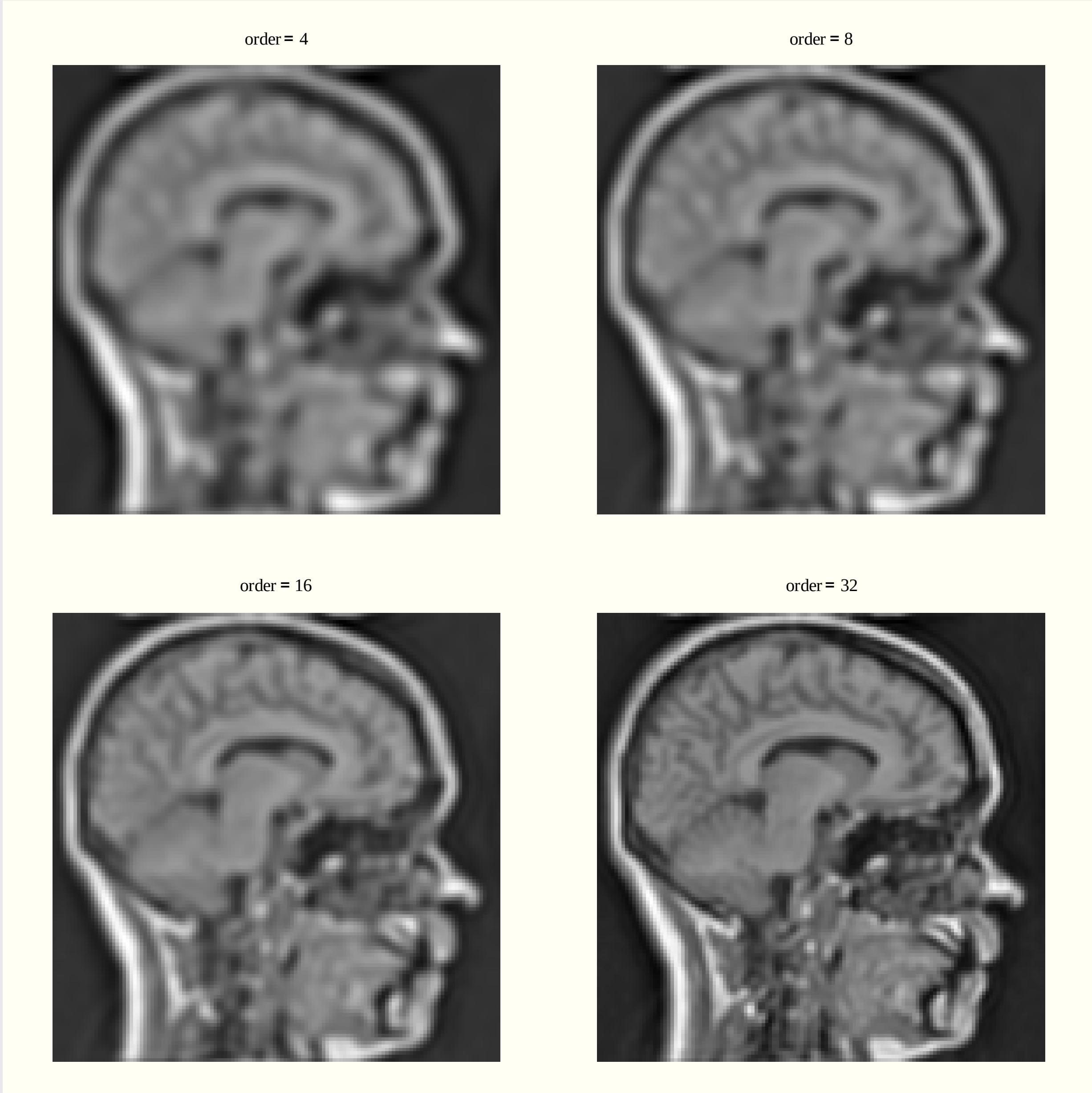

12th order Laplacian = 24th order Gaussian derivatives

Out[20]=

```
0 4. gD im, 0., 2., 2. . gD im, 2., 0., 2. .
 8. gD im, 0., 4., 2. . 2. gD im, 2., 2., 2. . gD im, 4., 0., 2. 0
 10.6667 gD im, 0., 6., 2. . 3. gD im, 2., 4., 2. . 3. gD im, 4., 2., 2. . gD im, 6., 0., 2. .
 10.6667 gD im, 0., 8., 2. . 4. gD im, 2., 6., 2. .
    6. gD im, 4., 4., 2. . 4. gD im, 6., 2., 2. . gD im, 8., 0., 2. 0
 8.53333 gD im, 0., 10., 2. . 5. gD im, 2., 8., 2. . 10. gD im, 4., 6., 2. .
    10. gD im, 6., 4., 2. . 5. gD im, 8., 2., 2. . gD im, 10., 0., 2. .
 5.68889 gD im, 0., 12., 2. . 6. gD im, 2., 10., 2. . 15. gD im, 4., 8., 2. .
    20. gD im, 6., 6., 2. . 15. gD im, 8., 4., 2. . 6. gD im, 10., 2., 2. . gD im, 12., 0., 2. 0
 3.25079 gD im, 0., 14., 2. . 7. gD im, 2., 12., 2. . 21. gD im, 4., 10., 2. .
    35. gD im, 6., 8., 2. . 35. gD im, 8., 6., 2. .
    21. gD im, 10., 4., 2. . 7. gD im, 12., 2., 2. . gD im, 14., 0., 2. .
 1.6254 gD im, 0., 16., 2. . 8. gD im, 2., 14., 2. . 28. gD im, 4., 12., 2. .
    56. gD im, 6., 10., 2. . 70. gD im, 8., 8., 2. . 56. gD im, 10., 6., 2. .
    28. gD im, 12., 4., 2. . 8. gD im, 14., 2., 2. . gD im, 16., 0., 2. 0 0.722399
  gD im, 0., 18., 2. . 9. gD im, 2., 16., 2. . 36. gD im, 4., 14., 2. . 84. gD im, 6., 12., 2. .
    126. gD im, 8., 10., 2. . 126. gD im, 10., 8., 2. . 84. gD im, 12., 6., 2. .
    36. gD im, 14., 4., 2. . 9. gD im, 16., 2., 2. . gD im, 18., 0., 2. .
 0.288959 gD im, 0., 20., 2. . 10. gD im, 2., 18., 2. . 45. gD im, 4., 16., 2. .
    120. gD im, 6., 14., 2. . 210. gD im, 8., 12., 2. .
    252. gD im, 10., 10., 2. . 210. gD im, 12., 8., 2. . 120. gD im, 14., 6., 2. .
    45. gD im, 16., 4., 2. . 10. gD im, 18., 2., 2. . gD im, 20., 0., 2. 0
 0.105076 gD im, 0., 22., 2. . 11. gD im, 2., 20., 2. . 55. gD im, 4., 18., 2. .
    165. gD im, 6., 16., 2. . 330. gD im, 8., 14., 2. . 462. gD im, 10., 12., 2. .
    462. gD im, 12., 10., 2. . 330. gD im, 14., 8., 2. . 165. gD im, 16., 6., 2. .
    55. gD im, 18., 4., 2. . 11. gD im, 20., 2., 2. . gD im, 22., 0., 2. .
 0.0350254 gD im, 0., 24., 2. . 12. gD im, 2., 22., 2. . 66. gD im, 4., 20., 2. .
    220. gD im, 6., 18., 2. . 495. gD im, 8., 16., 2. . 792. gD im, 10., 14., 2. .
    924. gD im, 12., 12., 2. . 792. gD im, 14., 10., 2. . 495. gD im, 16., 8., 2. . 220.
     gD im, 18., 6., 2. . 66. gD im, 20., 4., 2. . 12. gD im, 22., 2., 2. . gD im, 24., 0., 2.
```

Colour receptive fields from eigenpatches of a color image

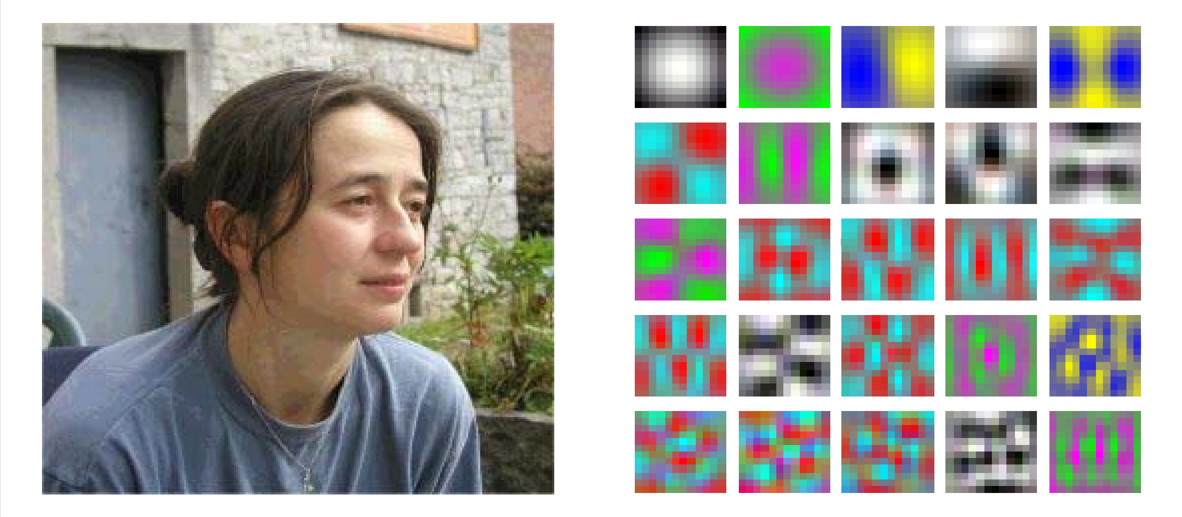

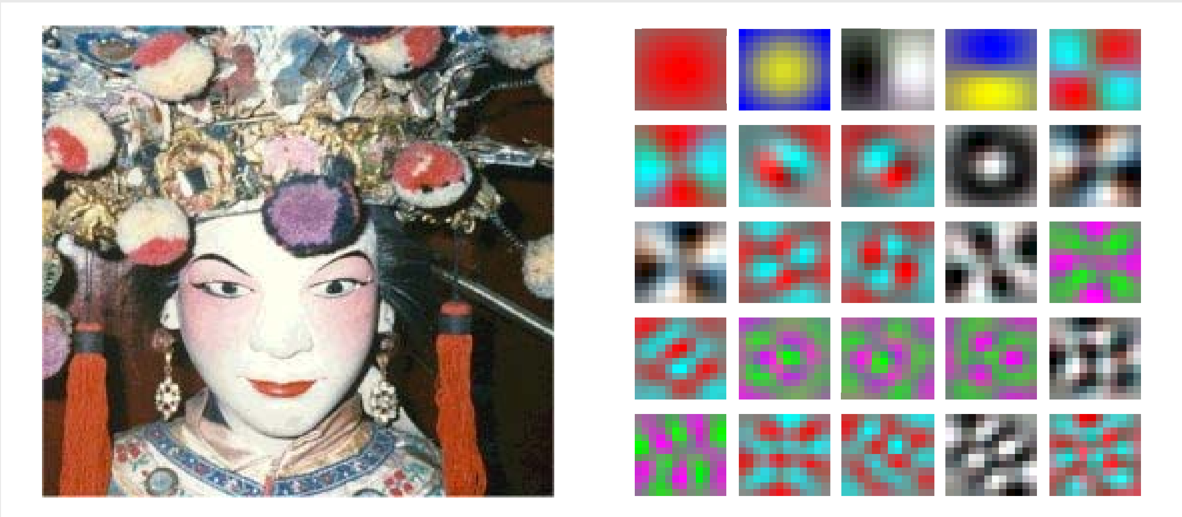

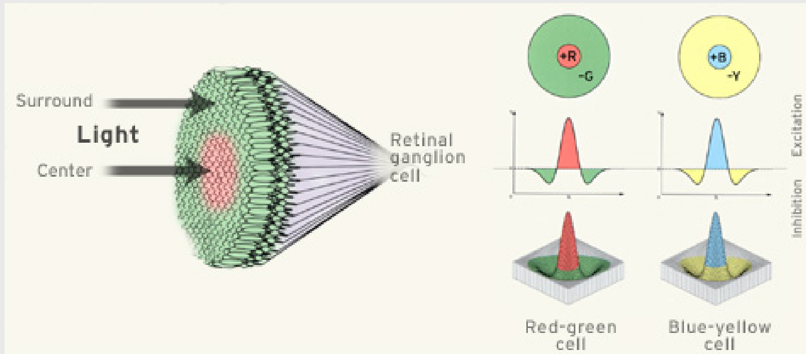

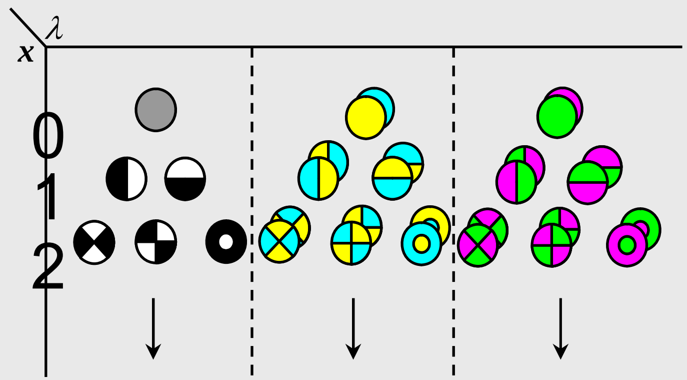

Lxux{!{nlny}r¡n:bnum|

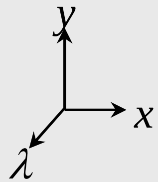

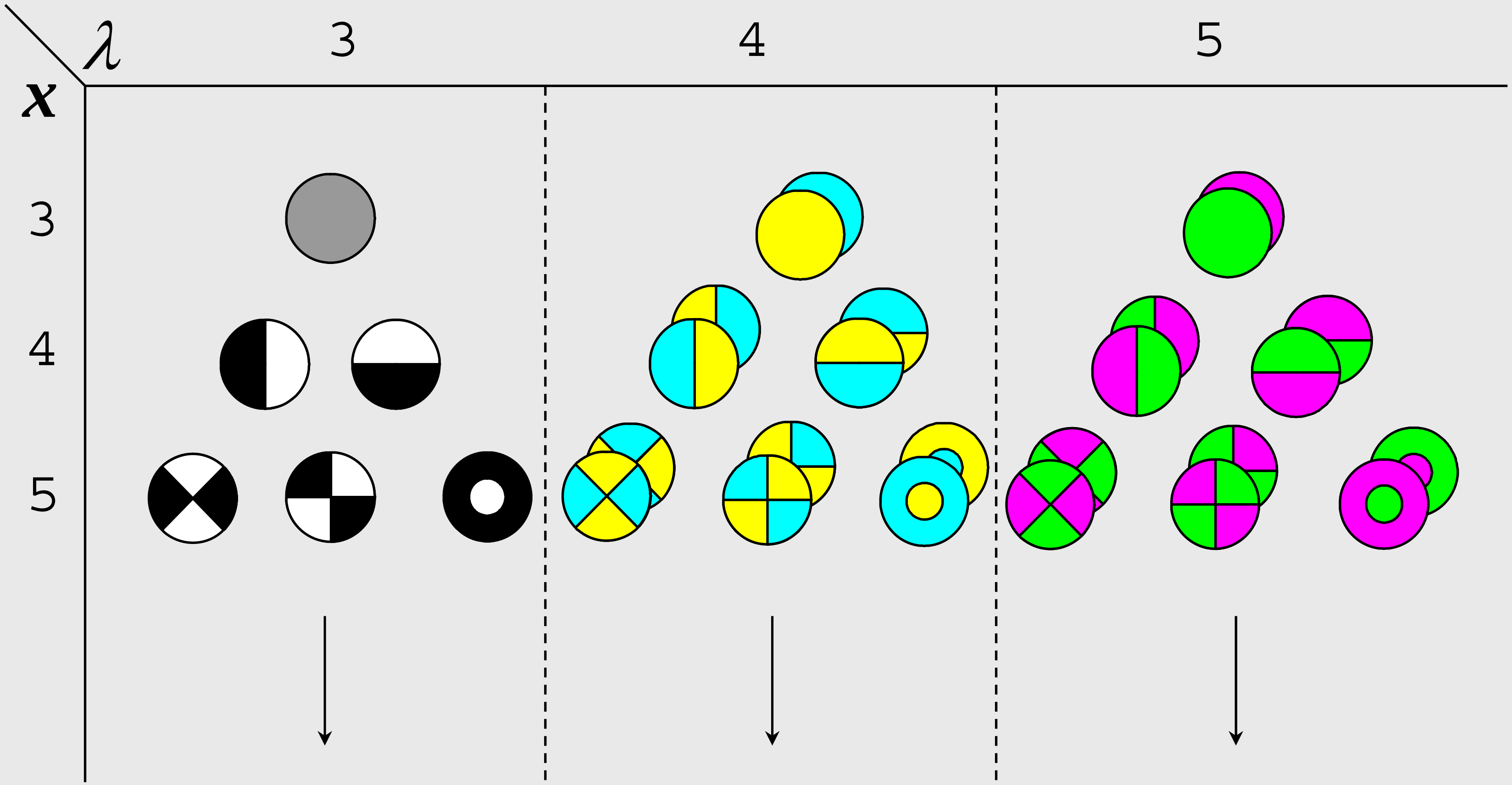

Hering basis

How can we *measure* color?

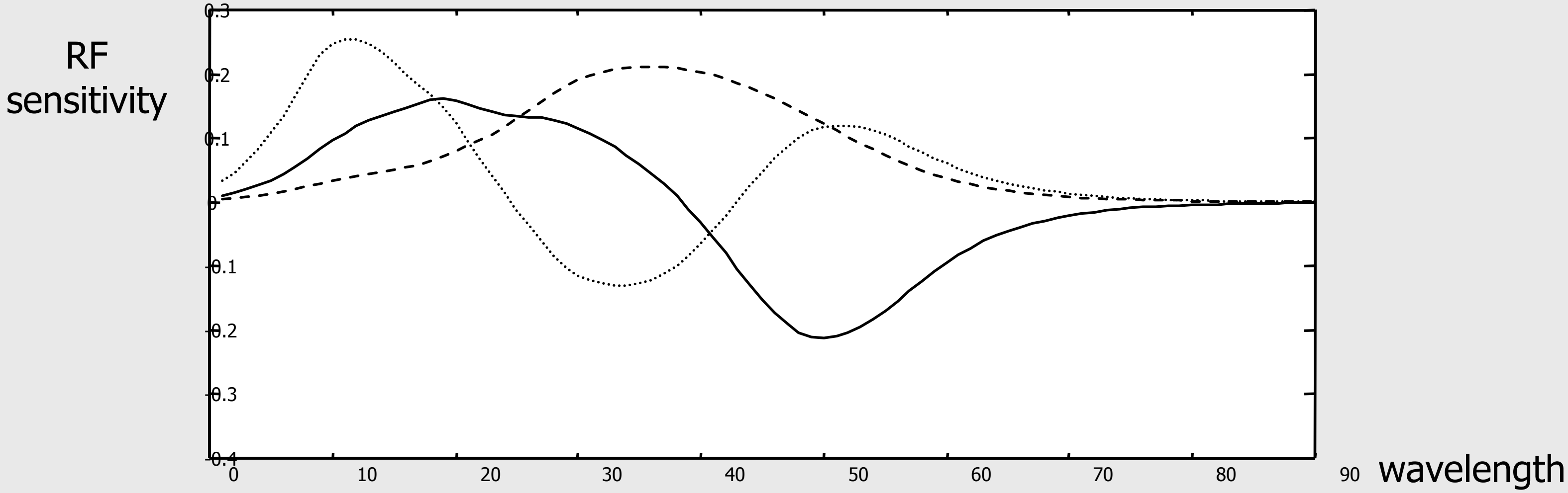

Idea Koenderink: *Gaussian derivatives* of zero, first and second order in the wavelength domain, single scale = 55 nm.

technische universiteit eindhoven

Lxwn!|nw|r}r;r}/

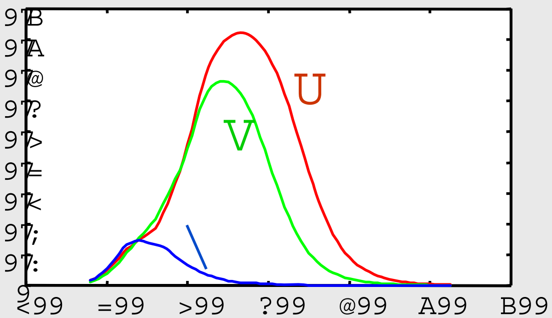

]j/ux{!lxux{!v xmnu

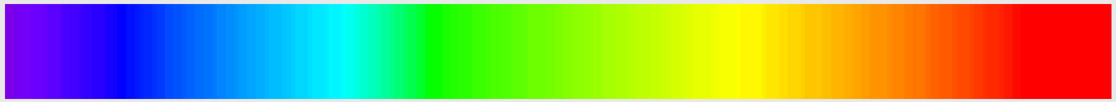

U~v mwjwln

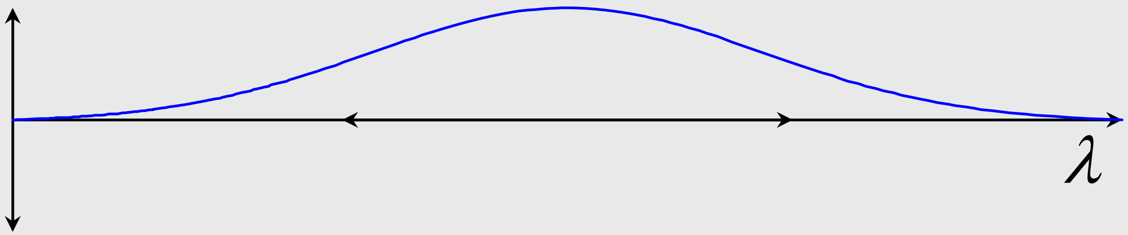

Ku-n6/nux¢wn||

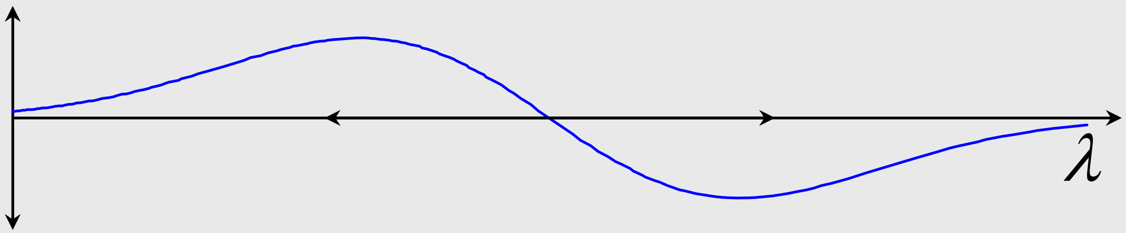

Y~{yun6p{nnwwn||

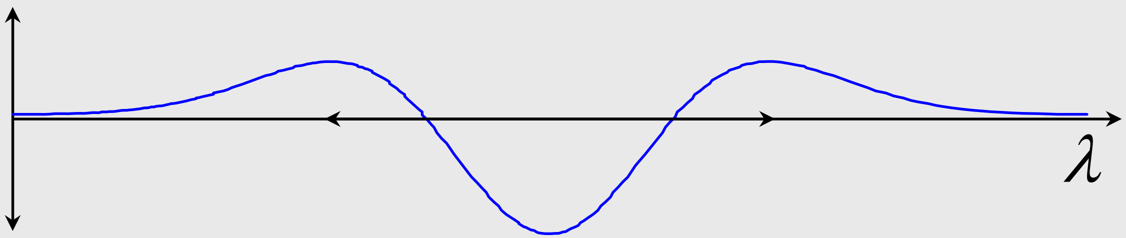

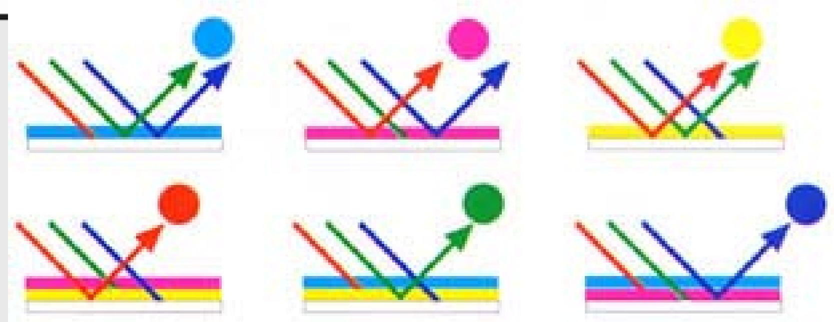

The reflected spectrum is:

$$E(\lambda) = e(\lambda)\,(1 - \rho_f(n,s,v))^2\; R_\infty(\lambda)$$

e(λ)= emitted light
v = viewing direction
n = surface patch normal
s = direction of illumination
ρ_f = Fresnel front surface reflectance coefficient
R_ = body reflectance

Because of projection of the energy distribution on the image plane the vectors n, s and v will depend on the position at the imaging plane. So the energy at a point x is then related to:

$$E(\lambda, x) = e(\lambda, x)(1 - \rho_f(x))^2 R_\infty(\lambda, x)$$

We assume an illumination with a locally constant color:

$$E(\lambda, x) = e(\lambda) i(x)(1 - \rho_f(x))^2 R_\infty(\lambda, x)$$

Aim: describe material changes independent of the illumination.

$$E(\lambda, x) = e(\lambda) i(x) (1 - \rho_f(x))^2 R_\infty(\lambda, x)$$

$$\frac{\partial E}{\partial \lambda} = i(x)(1 - \rho_f(x))^2 R_\infty(\lambda, x) \frac{\partial e}{\partial \lambda} + e(\lambda) i(x)(1 - \rho_f(x))^2 \frac{\partial R_\infty}{\partial \lambda}$$

Both equations have many common terms

The normalized differential

$$\hat{E} = \frac{1}{E}\frac{\partial E}{\partial \lambda} = \frac{1}{e(\lambda)}\frac{\partial e}{\partial \lambda} + \frac{1}{R_\infty(\lambda, x)}\frac{\partial R_\infty}{\partial \lambda}$$

determines material changes *independent of the viewpoint, surface orientation, illumination direction, illumination intensity and illumination color*!

The derivative jet to x and λ forms a complete family of geometric **invariants**:

$$\frac{\partial^{n+m}\hat{E}}{\partial\lambda^{n}\partial x^{m}}$$

These are *observed* properties, so we convolve with Gaussian derivatives

$$\frac{\partial^{n}\hat{E}}{\partial\lambda^{n}} = \hat{E}\otimes G(\lambda;\lambda_{0}\cong 515nm;\sigma_{\lambda}\cong 55nm)$$

Some color differential invariants

$E[im,\sigma]$	$E = \frac{1}{e}\frac{\partial e}{\partial \lambda}$	color invariant $\frac{1}{e}\frac{\partial e}{\partial \lambda}$
$E_{\lambda}[im,\sigma]$	$\frac{\partial E}{\partial \lambda}$	first wavelength derivative of E
$E_{\lambda\lambda}[im,\sigma]$	$\frac{\partial^2 E}{\partial \lambda^2}$	second wavelength derivative of E
$\gamma G[im,\sigma]$	$\sqrt{\left(\frac{\partial E}{\partial x}\right)^2 + \left(\frac{\partial E}{\partial y}\right)^2}$	yellow-blue edges
$\gamma W[im,\sigma]$	$\sqrt{\left(\frac{\partial E}{\partial x \partial \lambda}\right)^2 + \left(\frac{\partial E}{\partial y \partial \lambda}\right)^2}$	red-green edges
$\gamma N[im,\sigma]$	$\sqrt{\left(\frac{\partial E}{\partial x}\right)^2 + \left(\frac{\partial E}{\partial y}\right)^2 + \left(\frac{\partial E}{\partial x \partial \lambda}\right)^2 + \left(\frac{\partial E}{\partial y \partial \lambda}\right)^2}$	total color edge strength

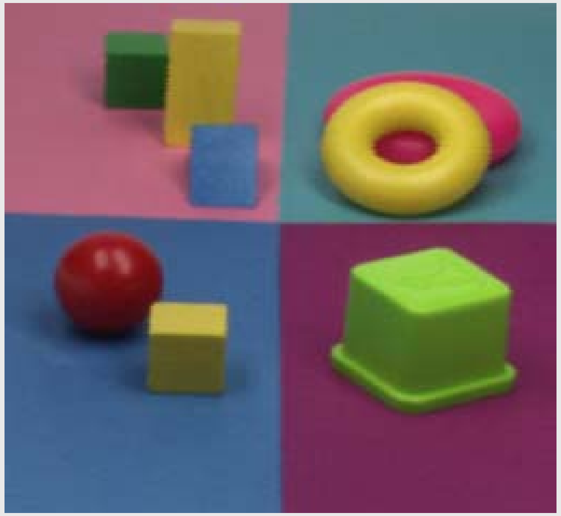

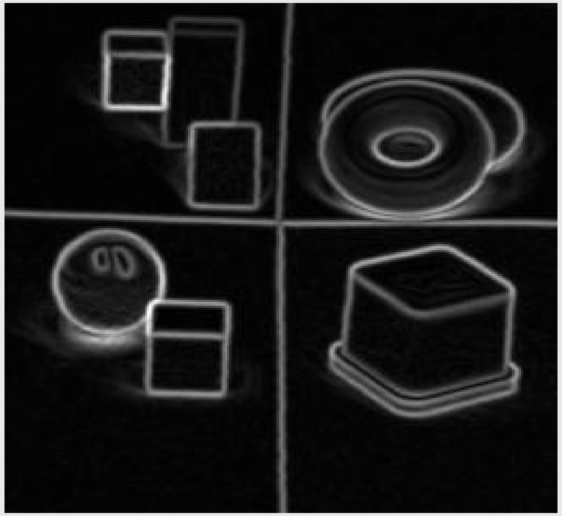

Luminance gradient
edge detection

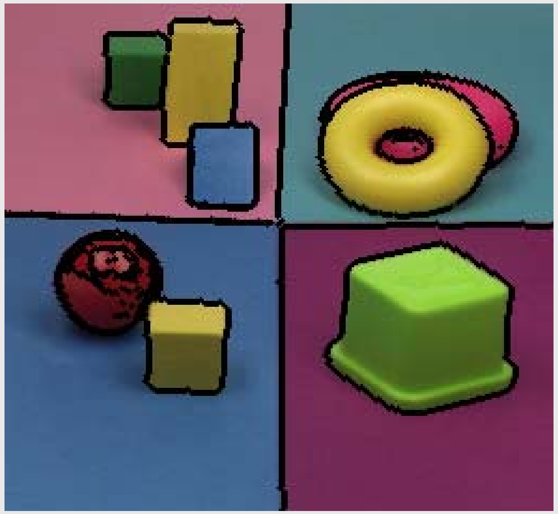

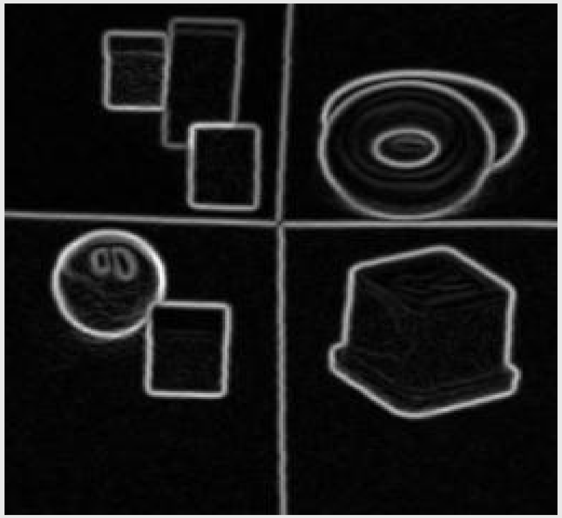

Color invariant
edge detection

Blue-yellow edges

Note the complete absence of detection of black-white edges.

technische universiteit eindhoven

Multi-orientation analysis

Orientation sensitivity map of simple cells in V1

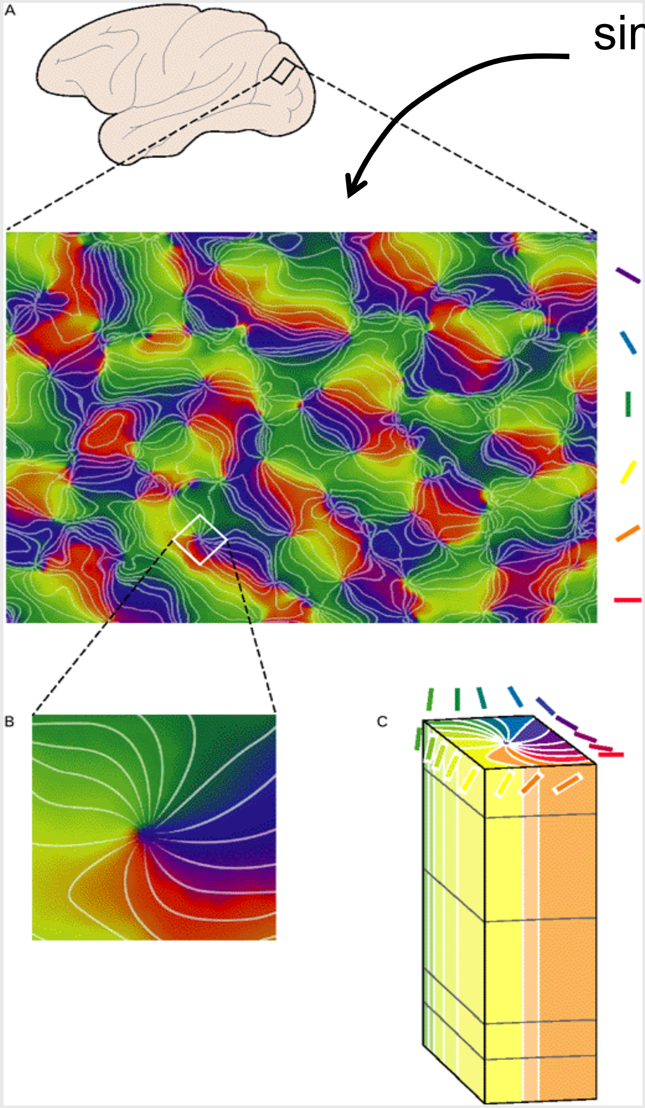

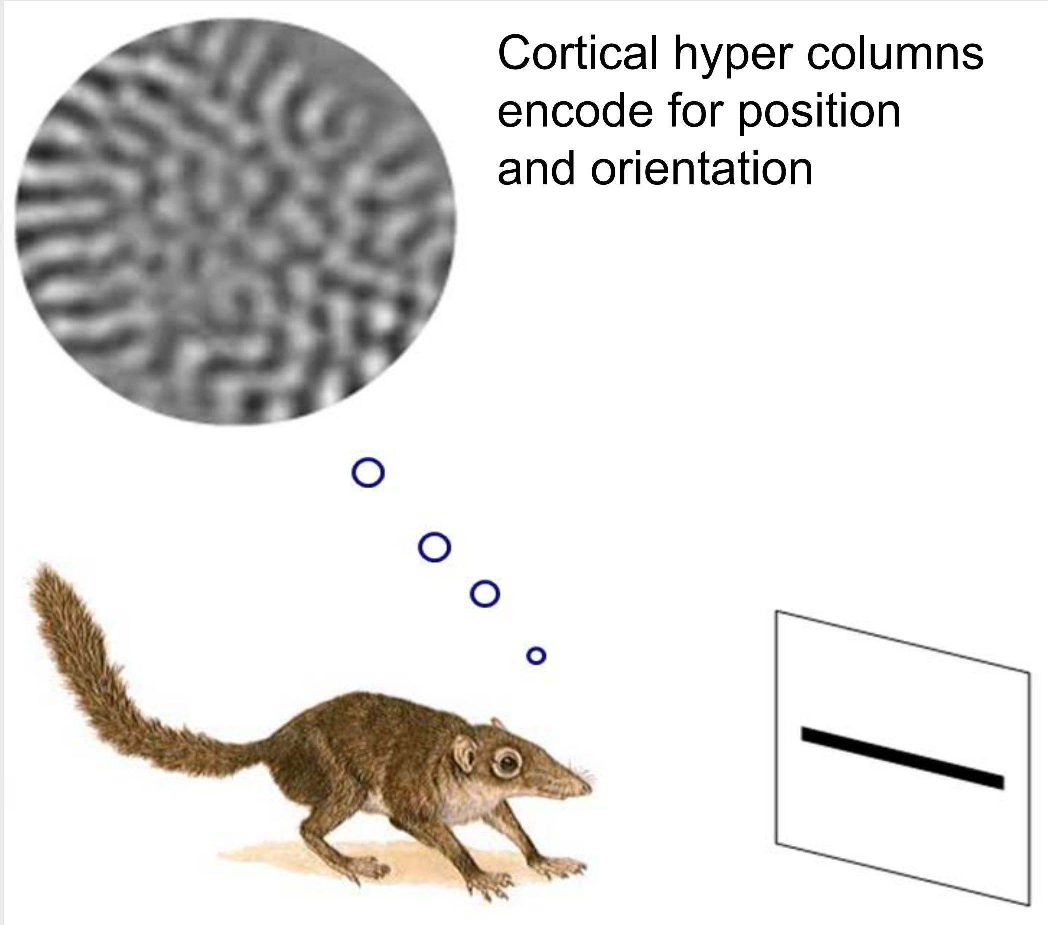

Hyper column with famous pinwheel structure

Connections exist between similar orientations to far away columns

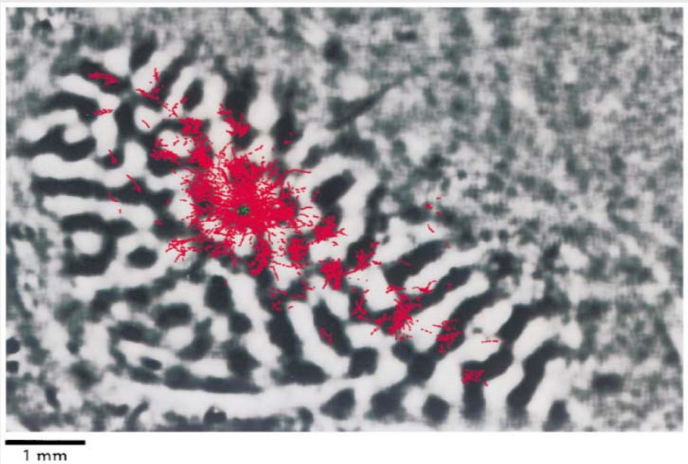

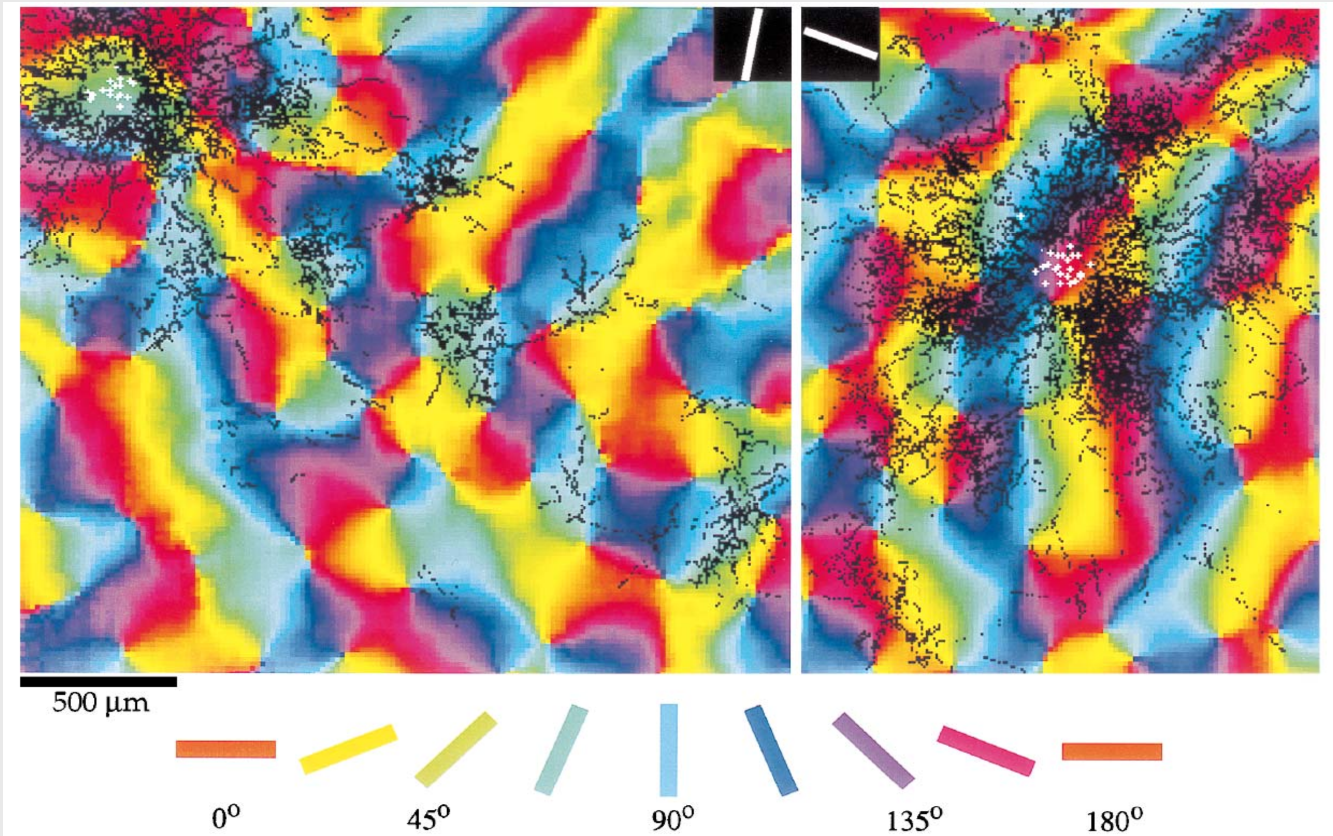

Fitzpatrick, Duke University, Nature 2002

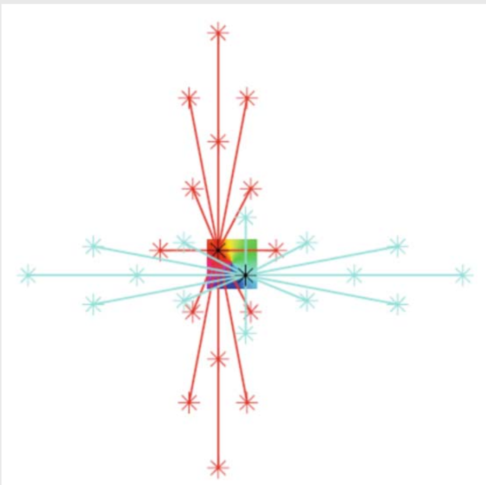

Alexander & van Leeuwen, 2010

Orientation scores model the cortical columns

A (pixel) column $U(x, y, \cdot)$ in an orientation score U models a cortical hypercolumn

Image

Orientation Score

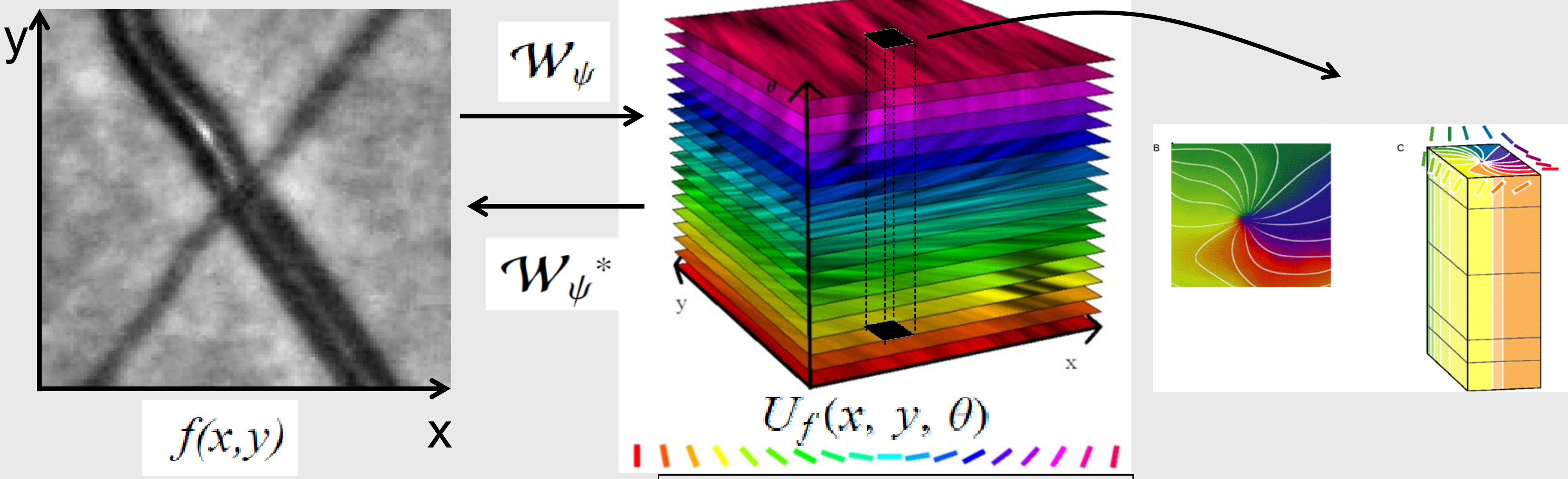

In an orientation score, crossing structures are disentangled.

Duits, R. Duits, M. Almsick, and B. Haar Romeny, “Invertible orientation scores as an application of generalized wavelet theory,” *Pattern Recognition and Image Analysis,* vol. 17, no. 1, pp. 42–75, Mar. 2007.

Oriented wavelets

Cake wavelets

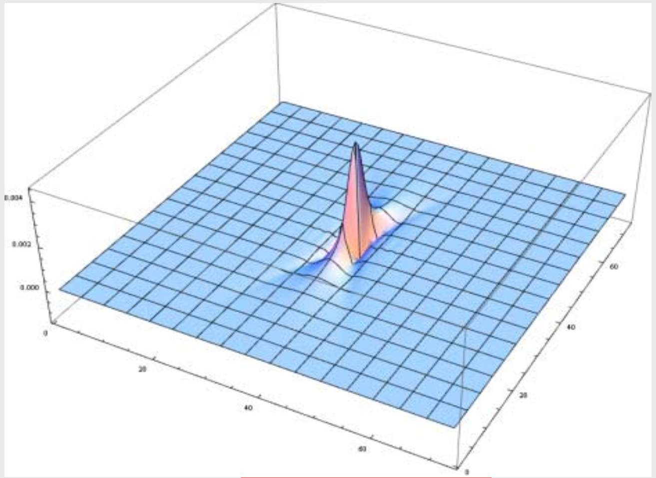

$$\psi^{cake}(\mathbf{x}) = \boxed{\mathcal{F}^{-1}[\boxed{\tilde{\psi}^{cake}}]}(\mathbf{x})G_{\sigma_s}(\mathbf{x})$$

Gabor wavelets

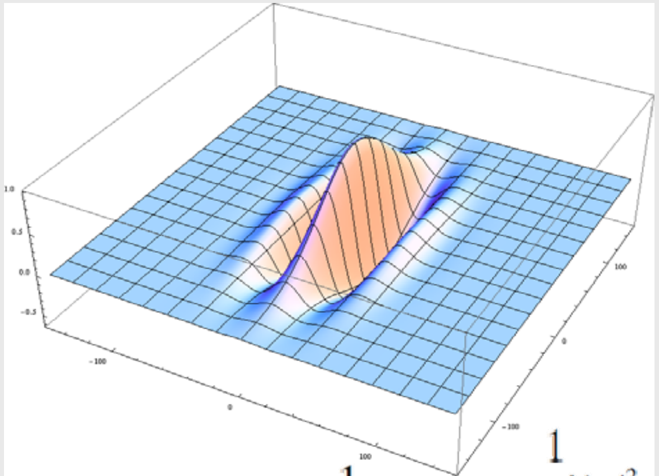

$$\psi^{gabor}(\mathbf{x}) = \frac{1}{C_\psi}\, e^{i\mathbf{k}_0\mathbf{x}}\, e^{-\frac{1}{2}|\mathbf{A}\mathbf{x}|^2}$$

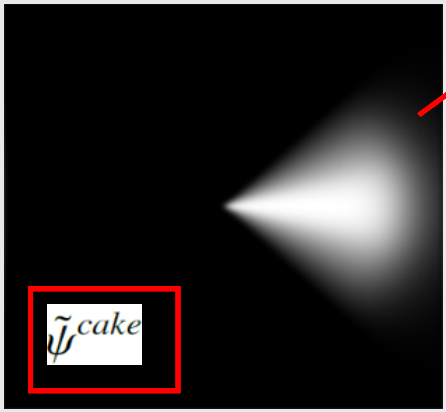

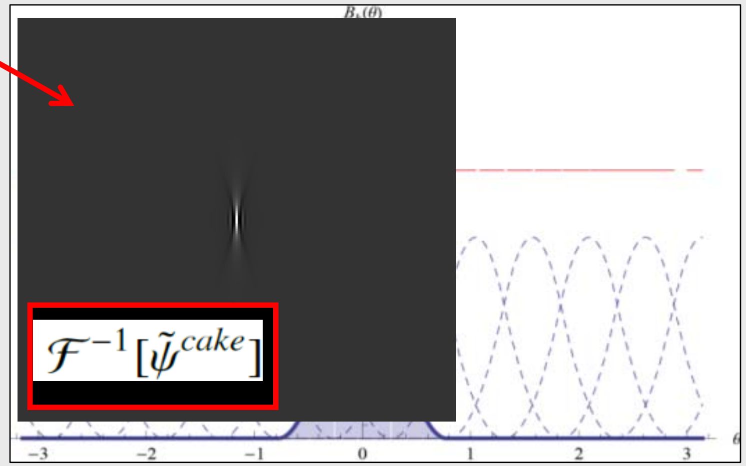

Sampling the Fourier domain in “pieces of a cake”

Oriented wavelets

Cake wavelets

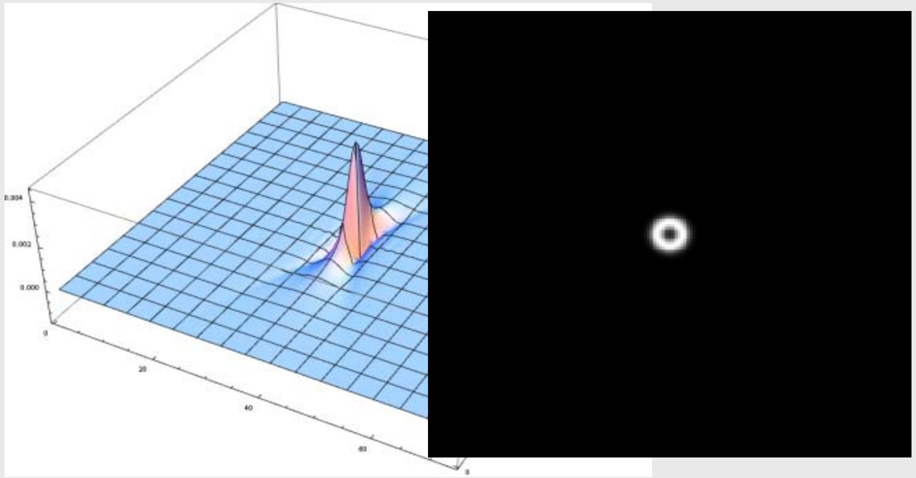

$$\psi^{cake}(\mathbf{x}) = \mathcal{F}^{-1}[\tilde{\psi}^{cake}](\mathbf{x})G_{\sigma_s}(\mathbf{x})$$

Gabor wavelets

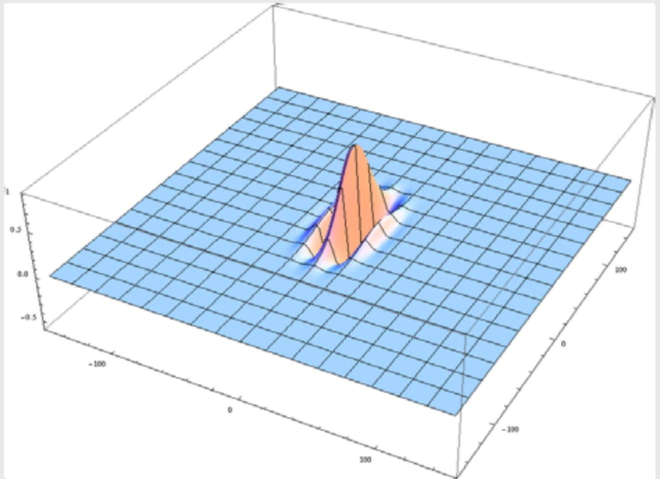

$$\psi^{gabor}(\mathbf{x}) = \frac{1}{C_\psi}\boxed{e^{i\mathbf{k}_0\mathbf{x}}}\boxed{e^{-\frac{1}{2}|A\mathbf{x}|^2}}$$

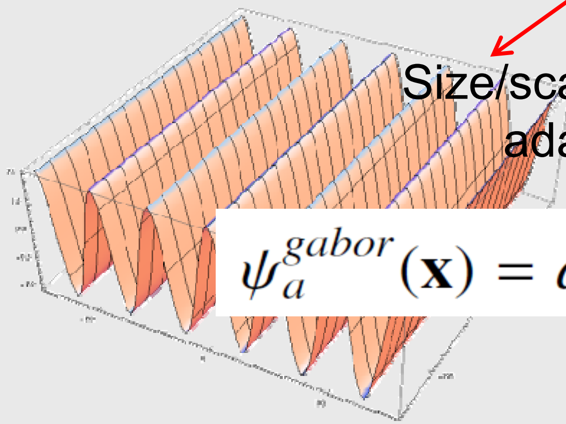

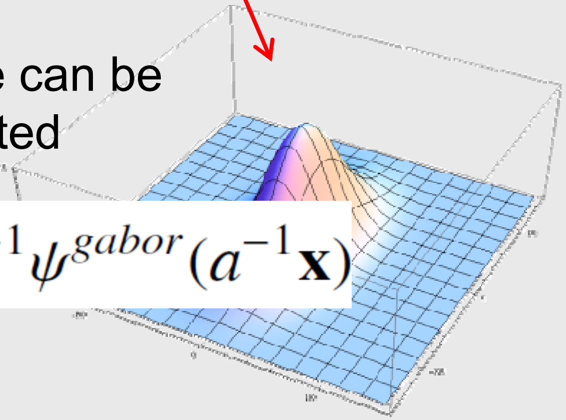

Size/scale can be adapted

$$\psi_a^{gabor}(\mathbf{x}) = a^{-1}\psi^{gabor}(a^{-1}\mathbf{x})$$

Orientation Scores: Gabor vs Cake Kernel

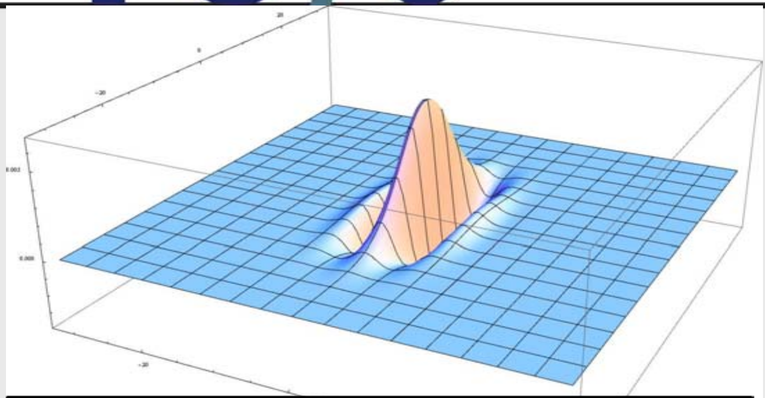

$$\frac{1}{2\pi\sigma_x\sigma_y} e^{-\frac{1}{2}\left(\frac{x^2}{\sigma_x^2}+\frac{y^2}{\sigma_y^2}\right)} e^{i2\pi f x}$$

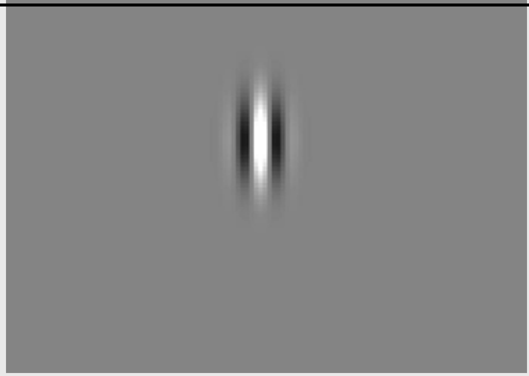

Gabor Kernel

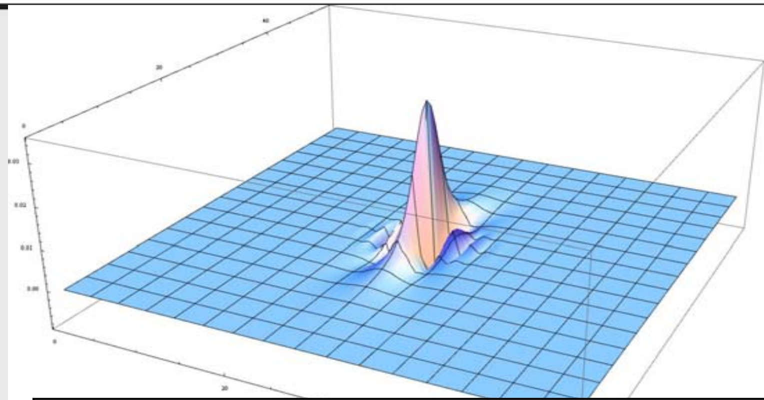

Duits et al. [1]

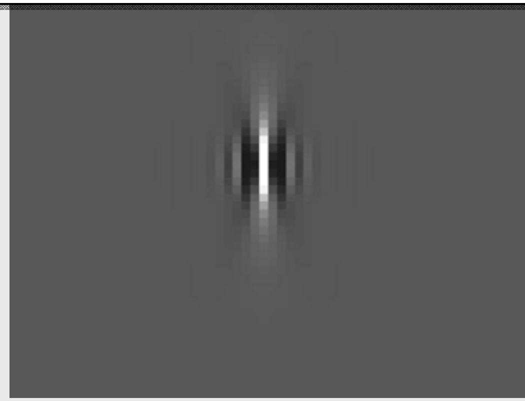

Cake Kernel

[1] R. Duits, M. Duits, M.A. van Almsick and B.M. ter Haar Romeny, “Invertible orientation scores as an application of generalized wavelet theory”, Pattern Recognition and Image Analysis (PRIA), vol. 17, no. 1, pp. 42-75, 2007

Gabor vs Cake Kernel – Fourier Domain

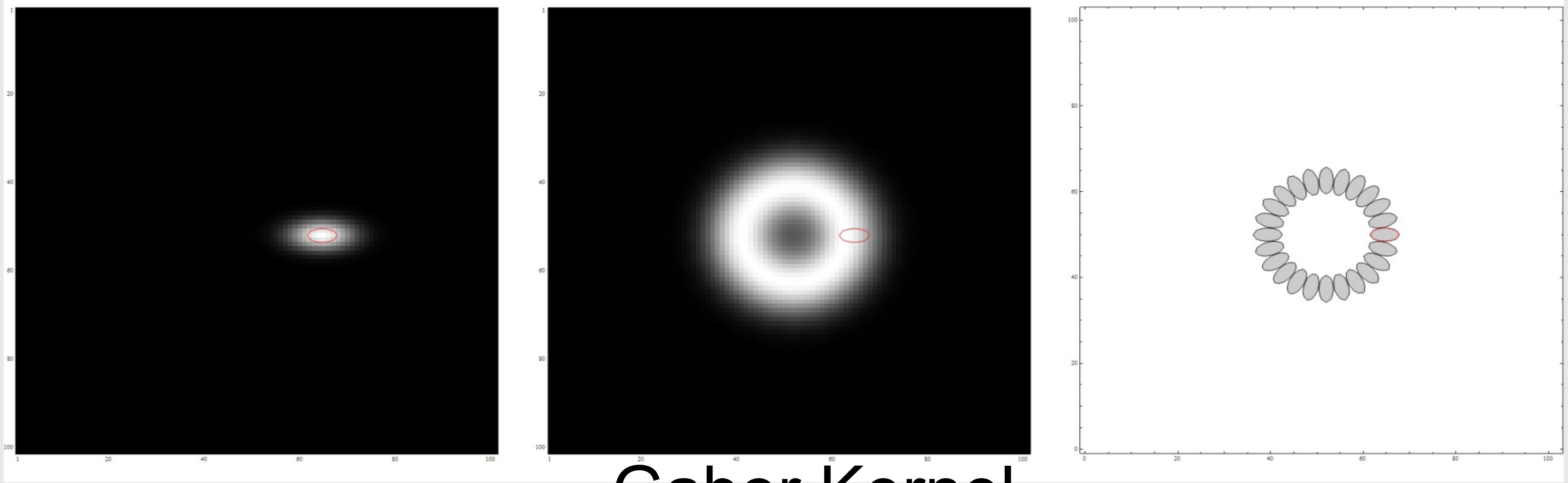

Gabor Kernel

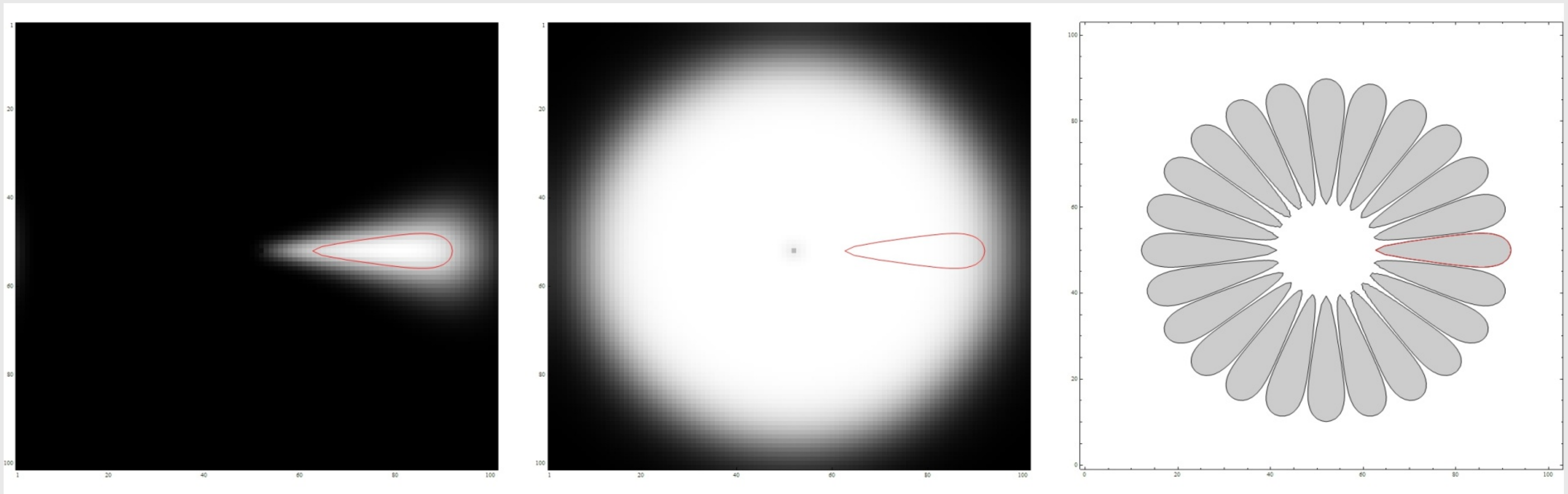

Cake Kernel

Construction of Orientation Scores

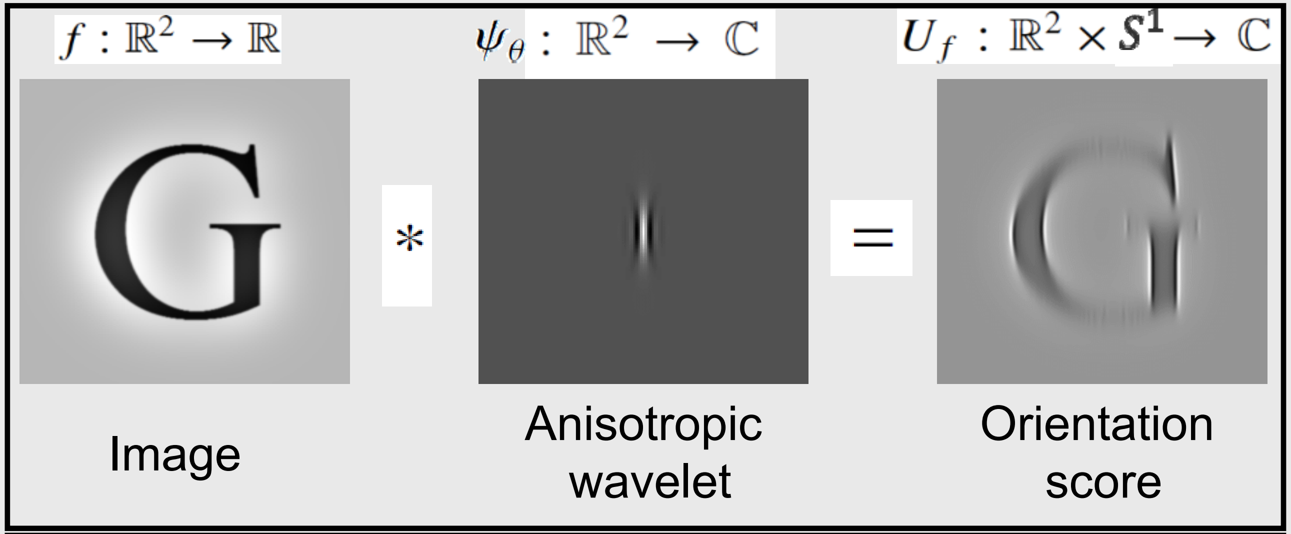

$$(f \quad * \quad \breve{\bar{\psi}}_\theta)(\mathbf{x}) = U_f(\mathbf{x},\theta)$$

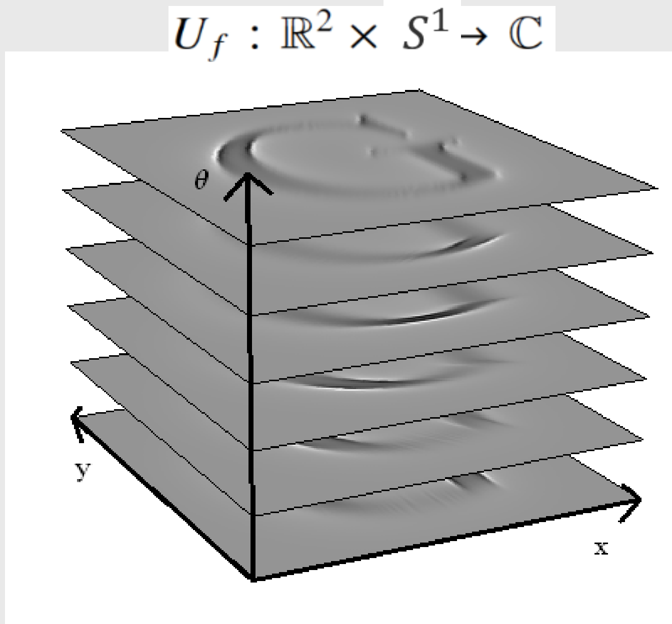

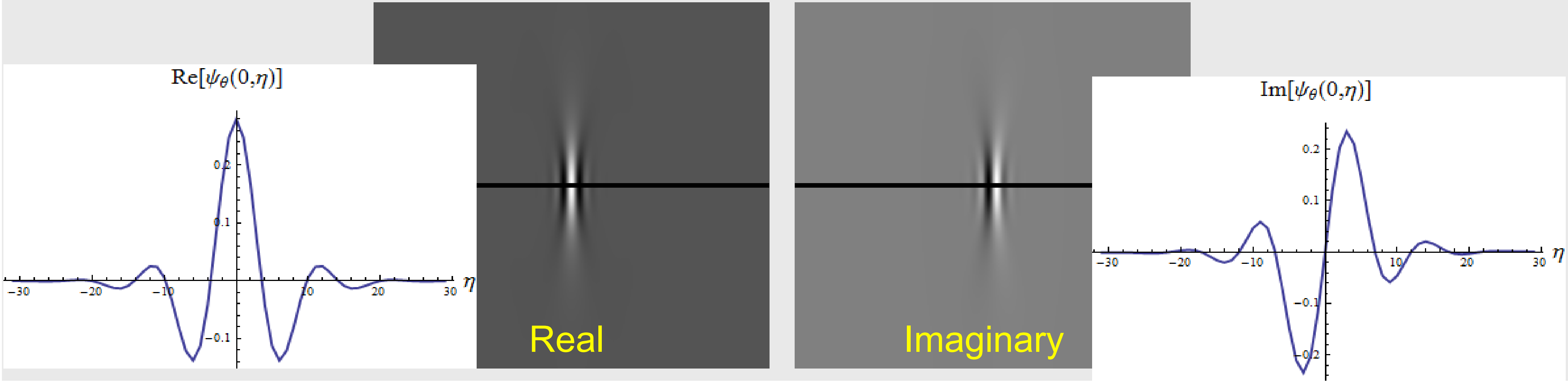

Jwrv j }rxw

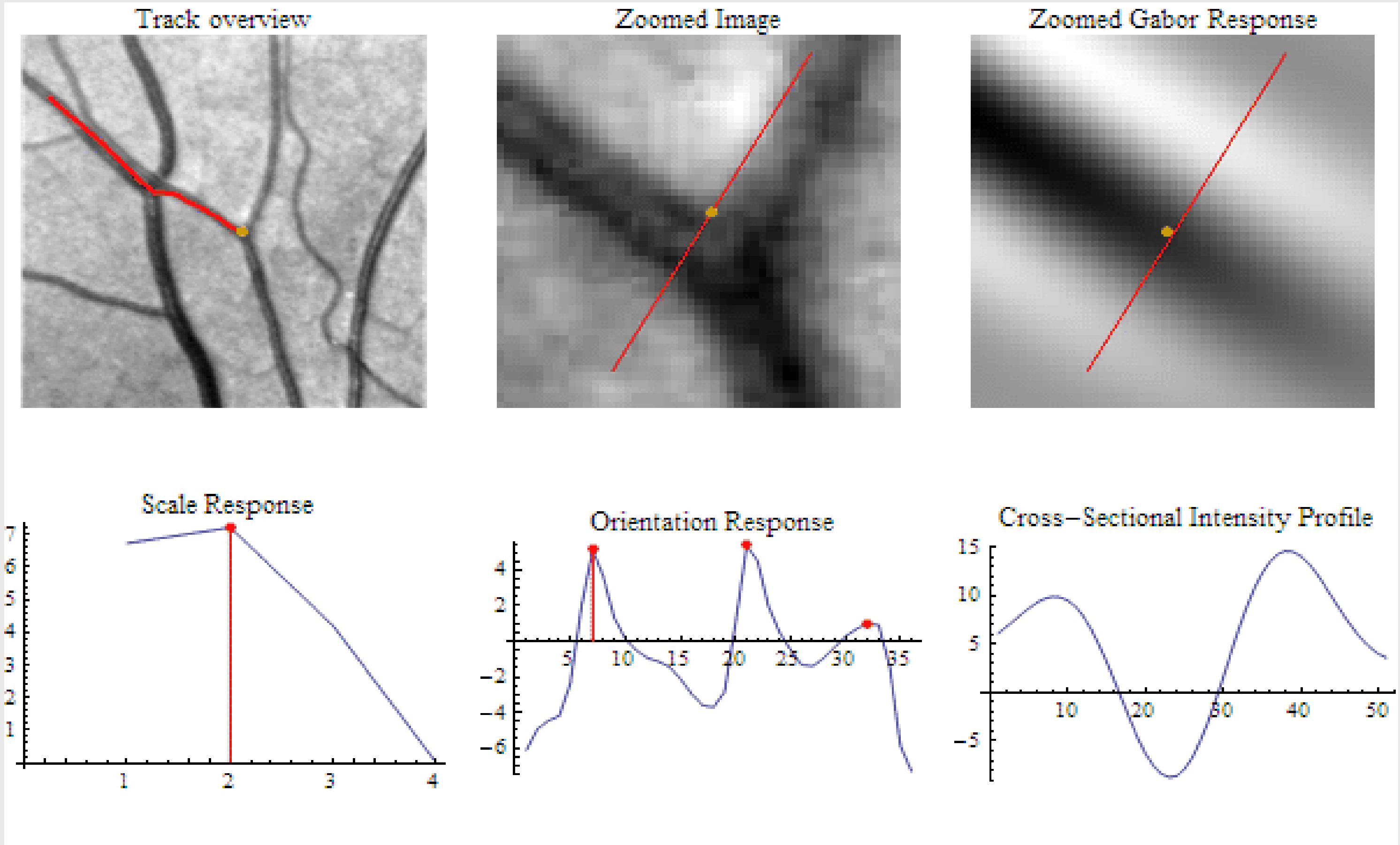
Track overview
Zoomed Image
Zoomed Gabor Response
Scale Response
Orientation Response
Cross–Sectional Intensity Profile

Jwrv j }rxw

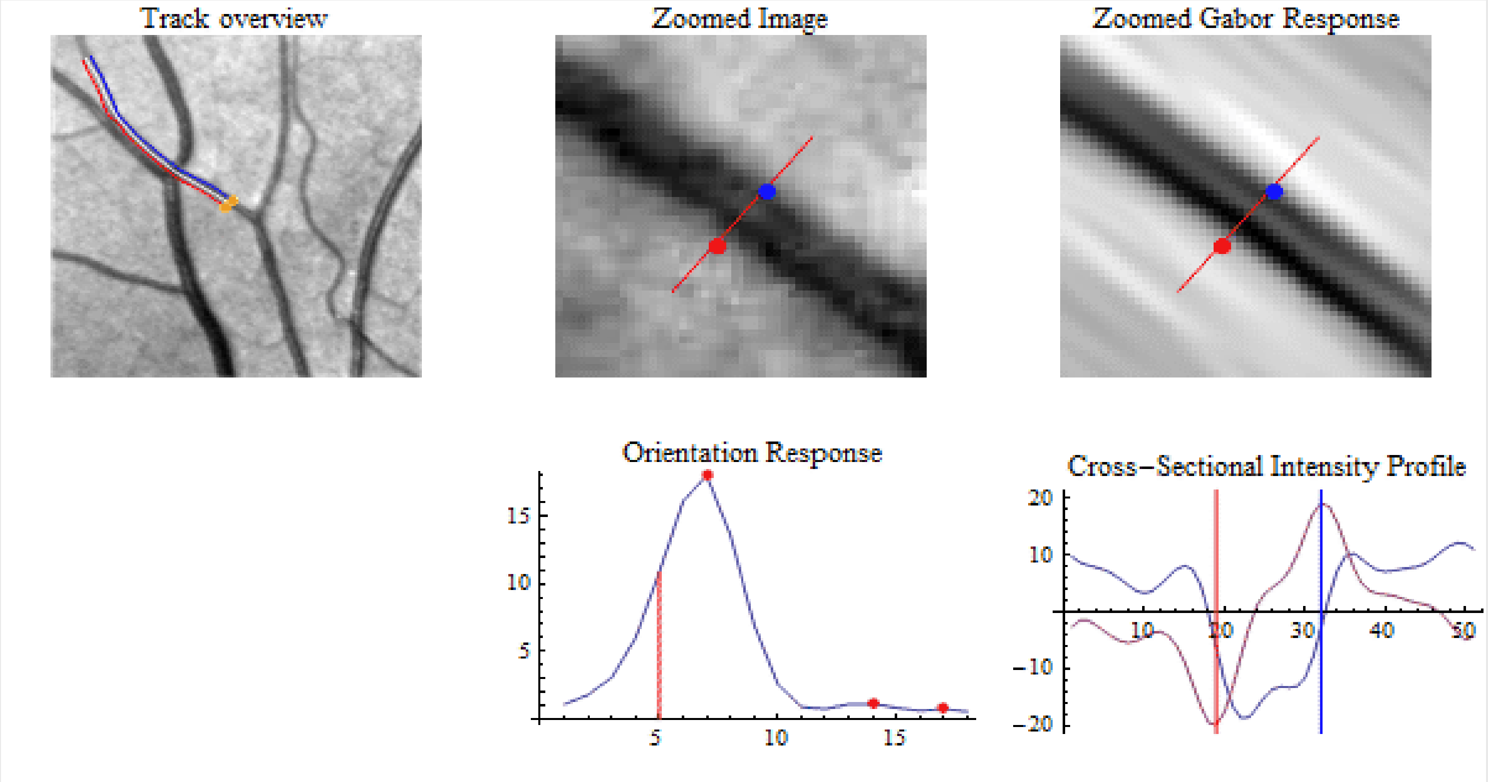
Track overview
Zoomed Image
Zoomed Gabor Response
Orientation Response
15
10
5
5
10
15
Cross−Sectional Intensity Profile
20
10
−10
−20
10
20
30
40
50

RetinaCheck.org

In China: 10% has diabetes, > 100 million people.
Massive screening program for early diabetes detection
TU/e + NEU: CAD on retinal fundus images.
Target: 24 million people (province of Liaoning).

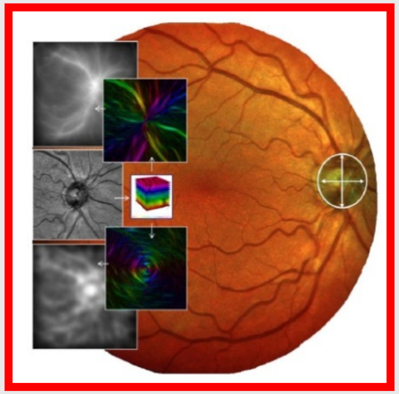

6 images 32 MB, 11 hospitals, 200 health centers, 4 vans
17 image features + 18 diabetic metadata
PR: SVM, LVQ, etc.

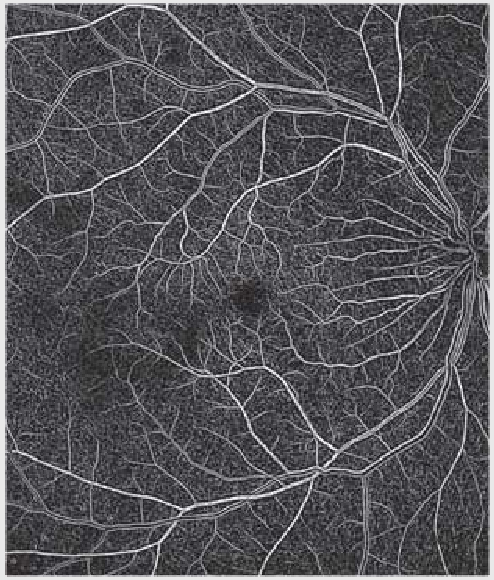

Maastricht Study: 5000+5000 people, 32 parameters, 38 M€/10y

With adaptive optics we can compensate for deformed wave fronts.
Now we can reveal individual photoreceptors.

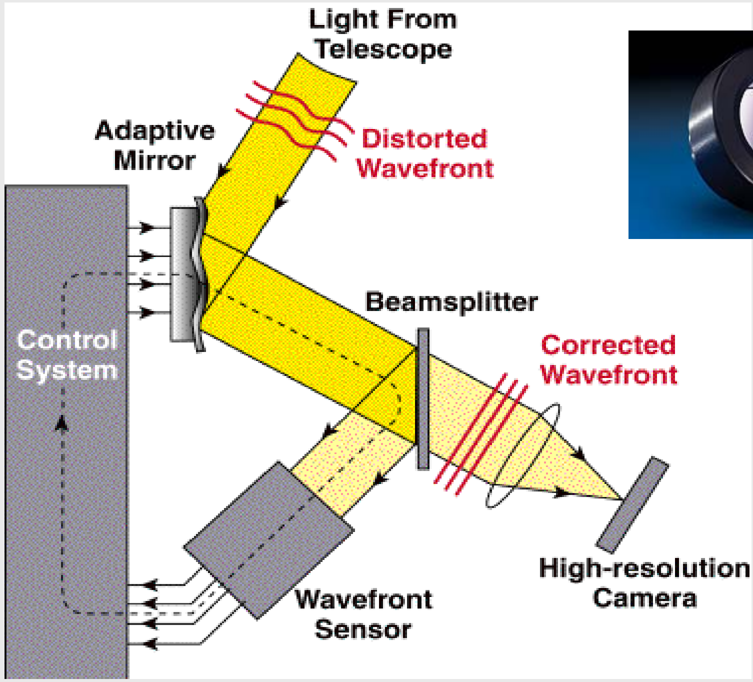

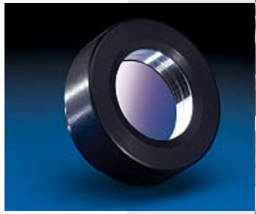

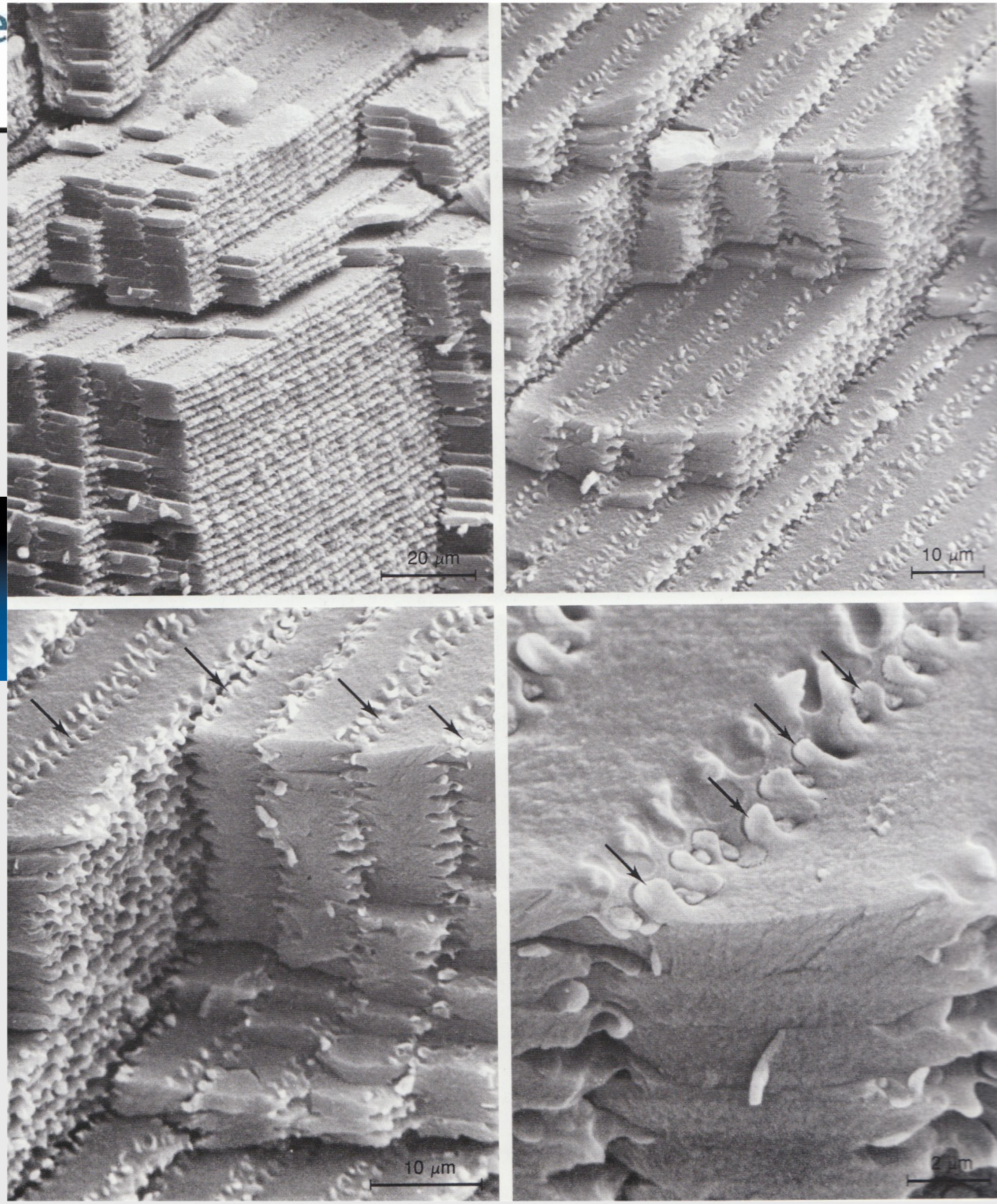

image

*

rotating
kernel

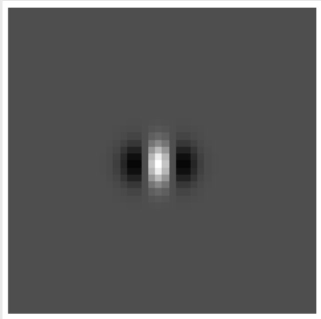

=

orientation space

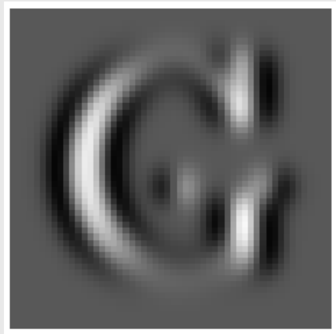

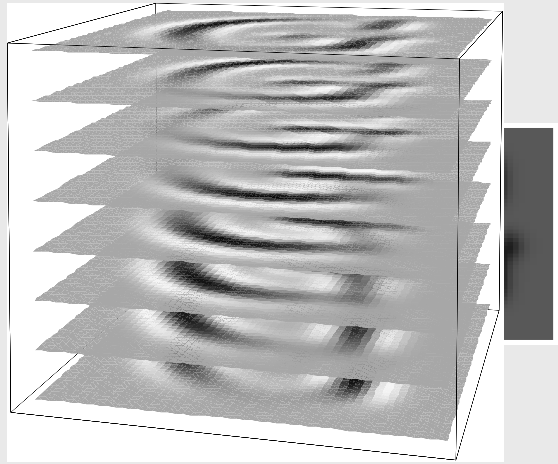

- Different orientations are disentangled in the orientation space

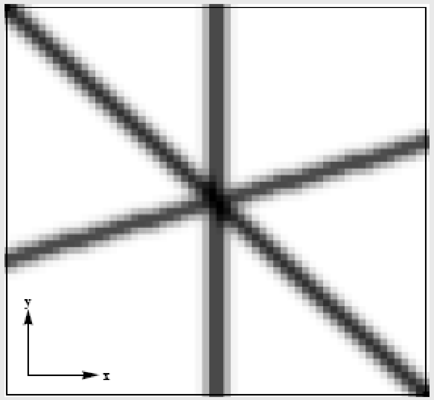

image

↔

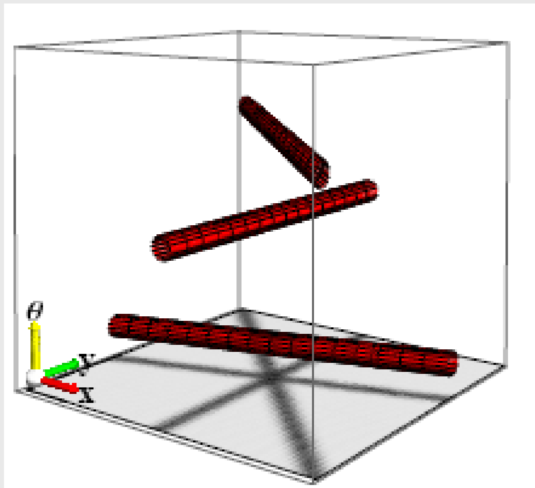

orientation score

Denoising of crossing fibers (collagen, tissue engineered heart valve)

Franken et al., TU/e, 2010

- **Operations on orientation scores**
  - **Diffusion on $\mathbb{R}^3 \times \mathbb{S}^2$**
    - **Contour enhancement**

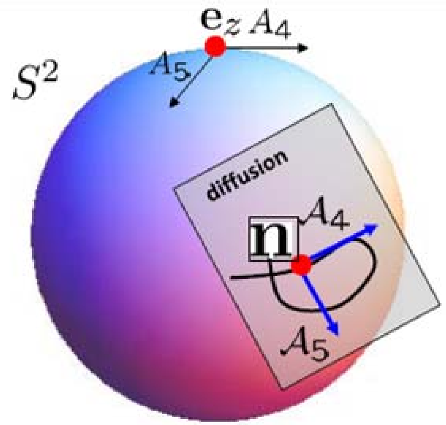

$$\partial_t W(\mathbf{x},\mathbf{n},t) = \left(D_{33}(\mathrm{A}_3)^2 + D_{44}((\boxed{\mathrm{A}_4})^2 + (\boxed{\mathrm{A}_5})^2) \right)$$

$$\lim_{t \downarrow 0} W(\mathbf{x},\mathbf{n},t) = U(\mathbf{x},\mathbf{n})$$

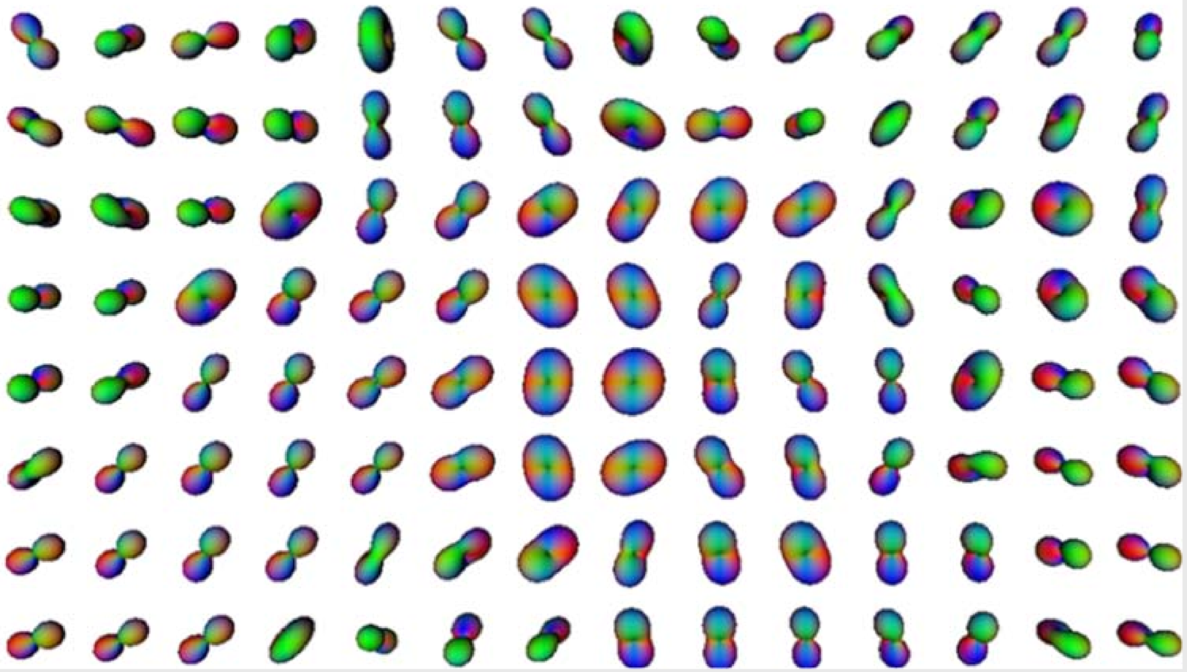

technische universiteit eindhoven

MRI: k-space: 3D spatial sampling, q-space: 3D orientational

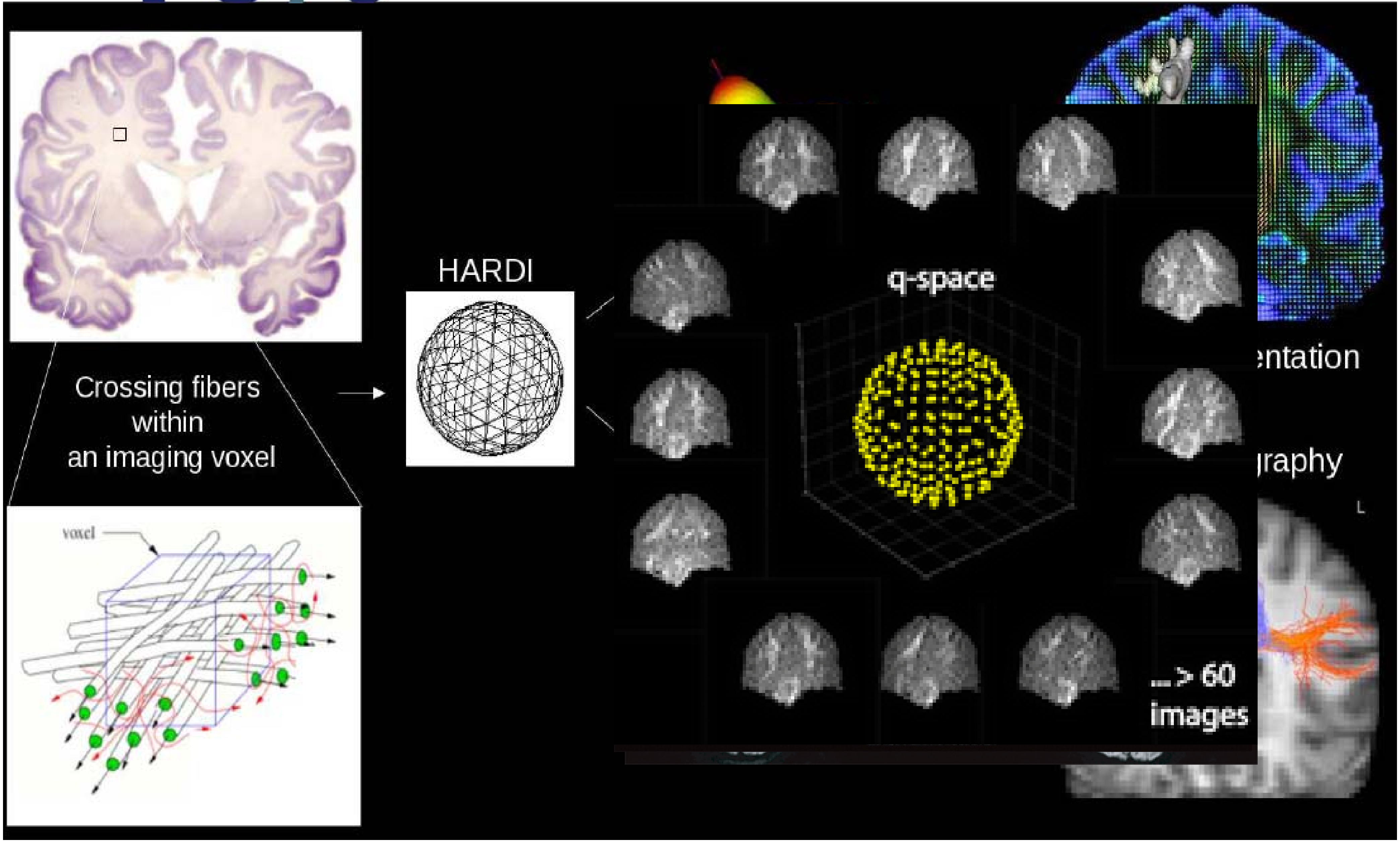

TU/e techni

The problem is crossings, kissings, splittings, endings, etc.
Glyphs: 8th order spherical harmonics

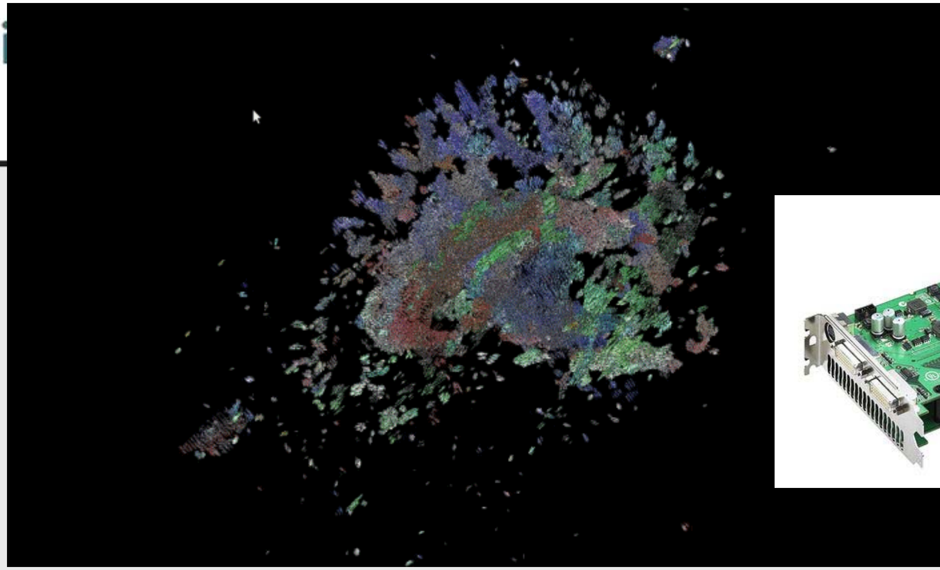

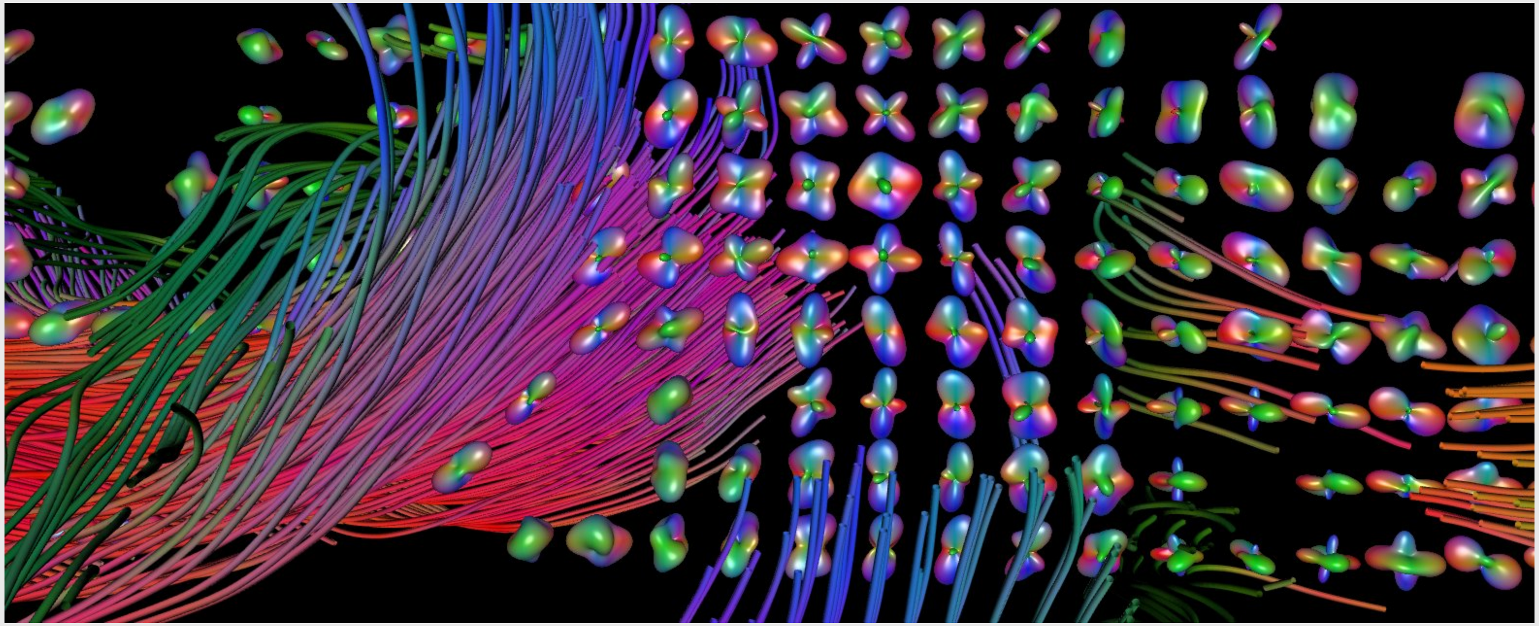

vIST/e: Visualization tool for DW MRI (A. Vilanova - project leader)

- **Operations on orientation scores**
  - **Diffusion on $\mathbb{R}^3 \times \mathbb{S}^2$**
    - **Linear contour enhancement: Convolution**

$$(\Phi(U))(\mathbf{x},\mathbf{n}) = \int_{\mathbb{R}^3}\int_{S^2} \boxed{p(R_{\mathbf{n}'}^T(\mathbf{x}-\mathbf{x}'), R_{\mathbf{n}'}^T\mathbf{n})}\, U(\mathbf{x}',\mathbf{n}')\, d\sigma(\mathbf{n}')\, d\mathbf{x}'$$

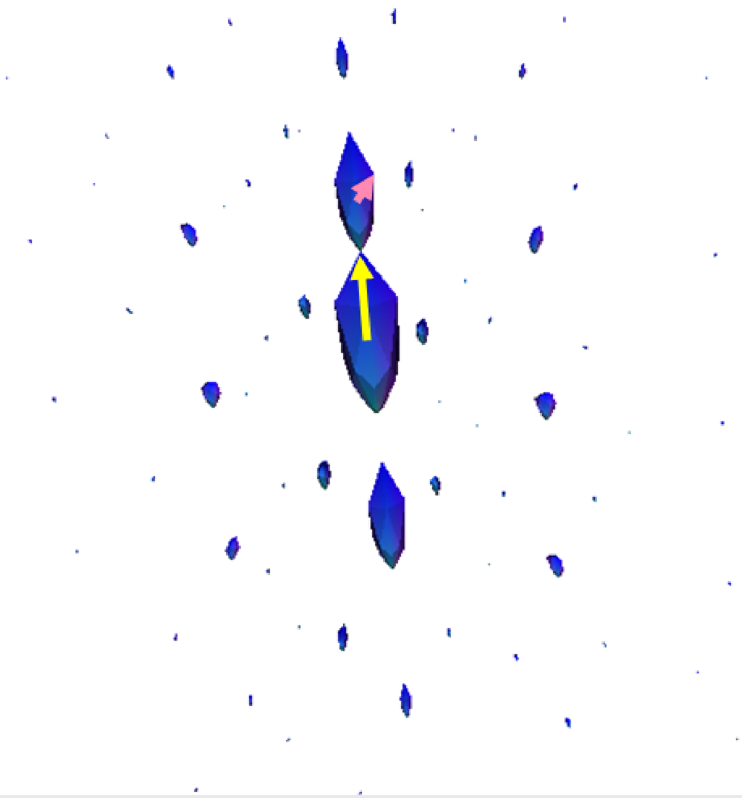

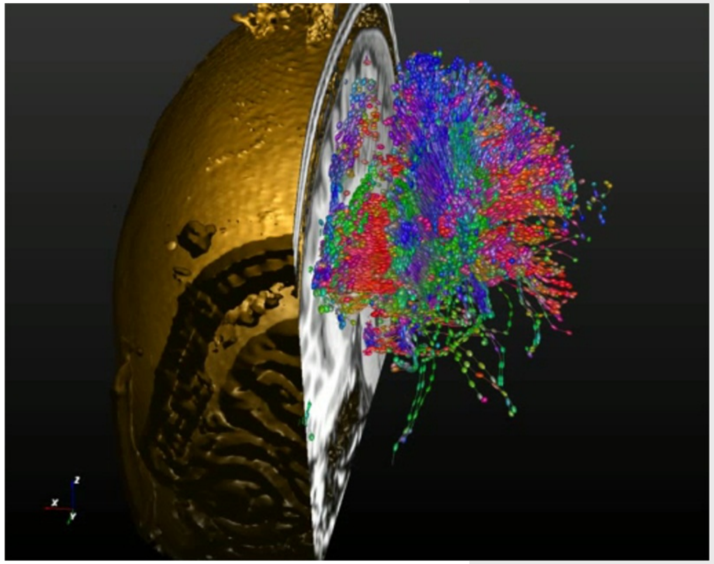

Complex brain connectivity from HARDI MRI sequences

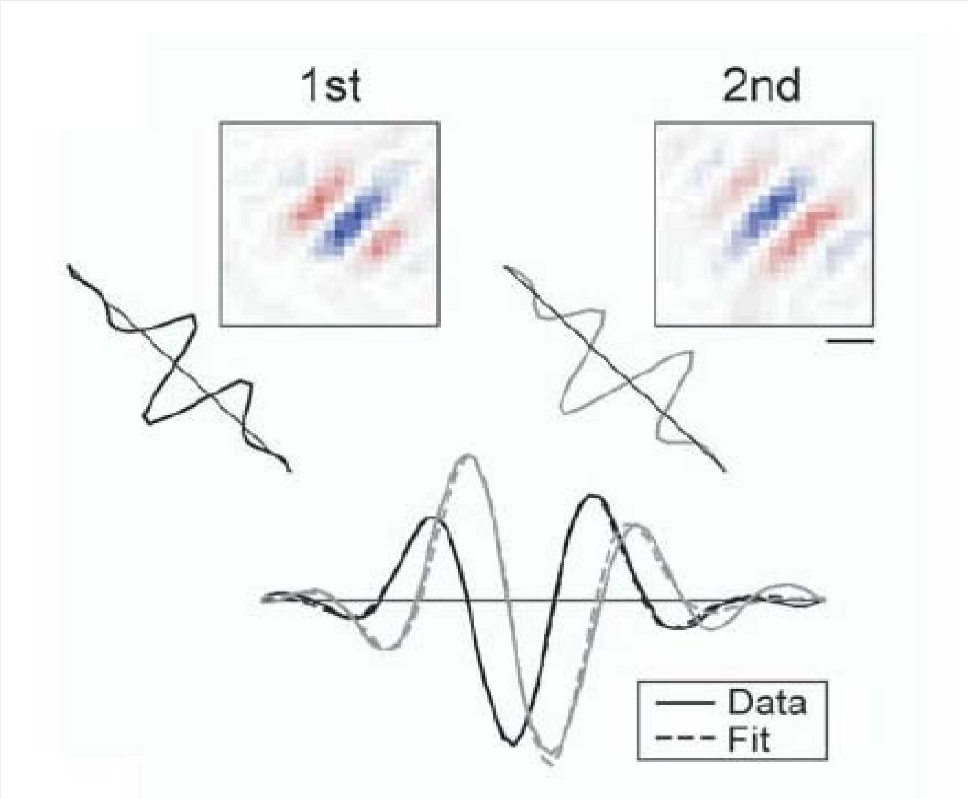

Gabor receptive fields
Gabor wavelets

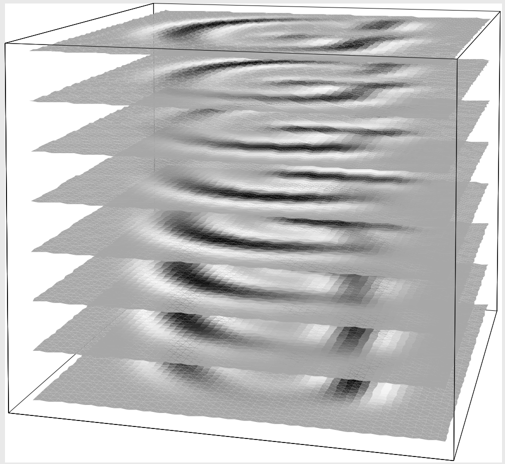

Multi-spatial frequency stack
(another filter bank)

Multi-spatial frequency

$$(\mathcal{W}_\psi f)(x,\omega,\phi) = \mathrm{e}^{-2\pi \mathrm{i}(\phi + \frac{x\omega}{2})} \int_{\mathbb{R}^d} f(\xi)\overline{\psi(\xi - x)}\mathrm{e}^{-2\pi \mathrm{i}(\xi - x)\omega}\,\mathrm{d}\xi$$

position phase

Score $U : (x, \omega, \phi) \mapsto (\mathcal{W}_\psi f)(x,\omega,\phi) \in \mathbb{R}$

frequency

$g = (x, \omega, \phi) \in H_r$ (Heisenberg group)

(Cf. $(x, \mathbf{R}_\vartheta) \in SE(d)$)

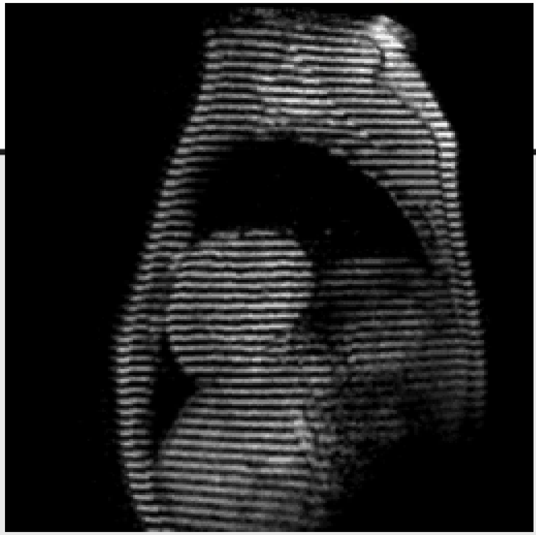

Cardiac deformation assessment – MRI tagging

thicker stripes: stretching

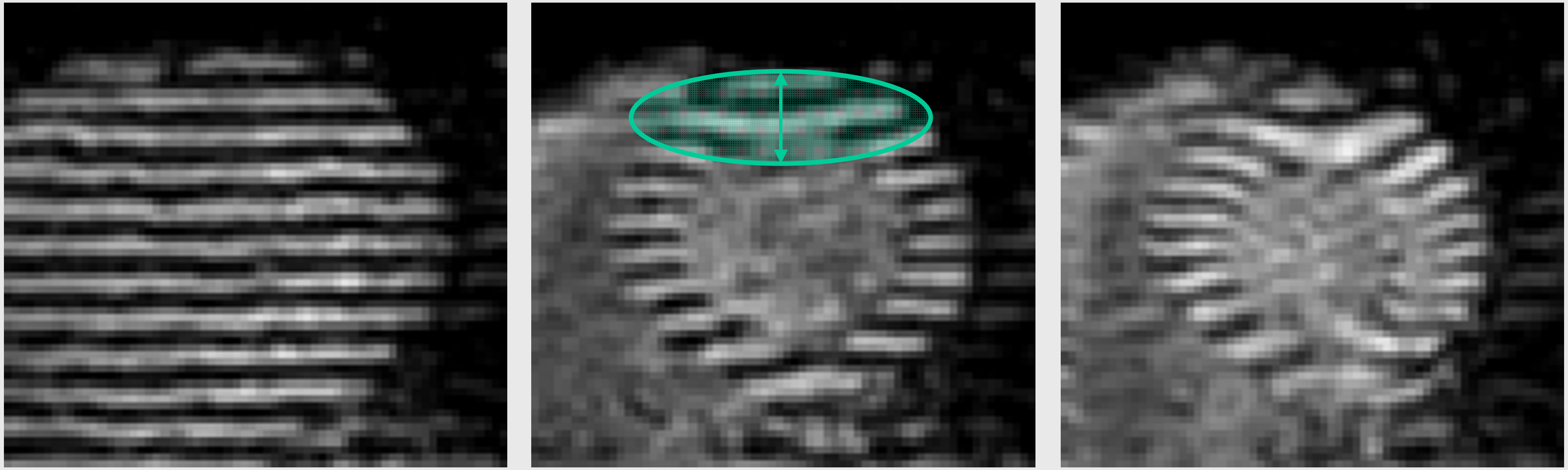

→ changes in local spatial frequency

Multi-spatial frequency – Gabor wavelets

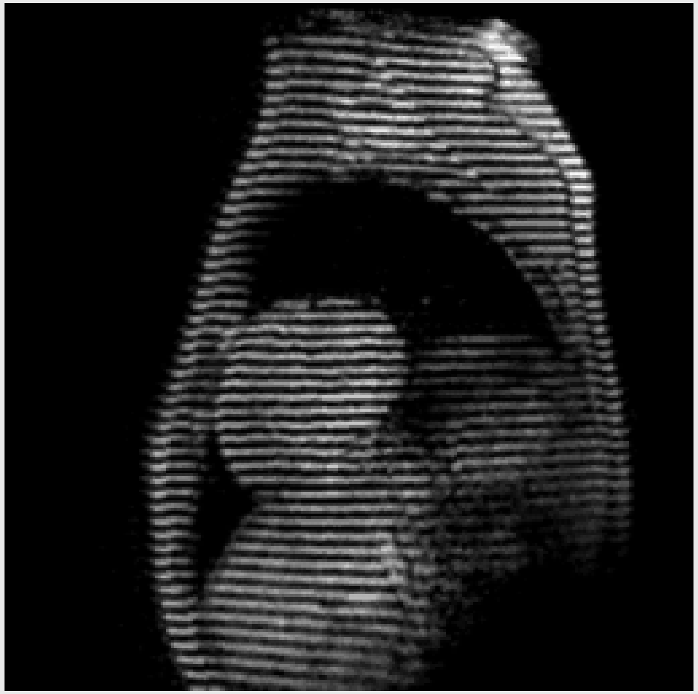

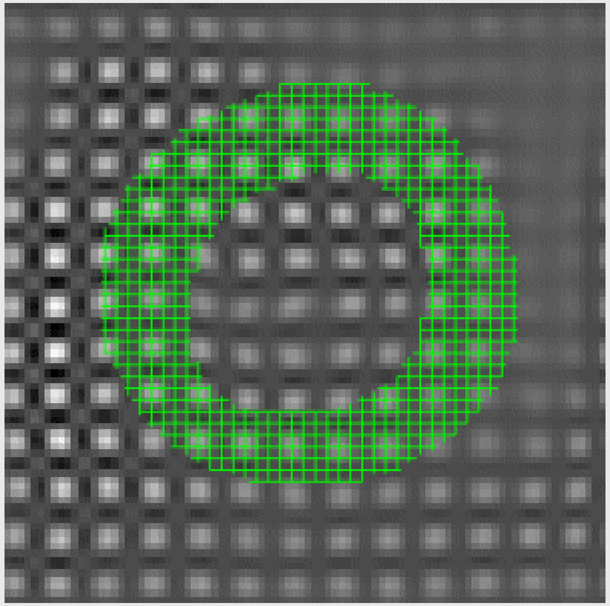

Non-invasive heart infarct quantification

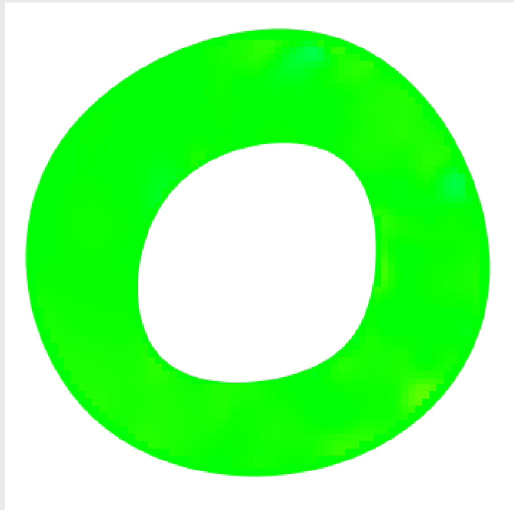

technische universiteit eindhoven

Math model for extensive filterbanks: Lie Group Vision

- Counter-intuitive: *add* dimensions
- Lie group theoretical model
- Axiomatic, first principles
  Context, Gestalt
- Massively parallel implementation

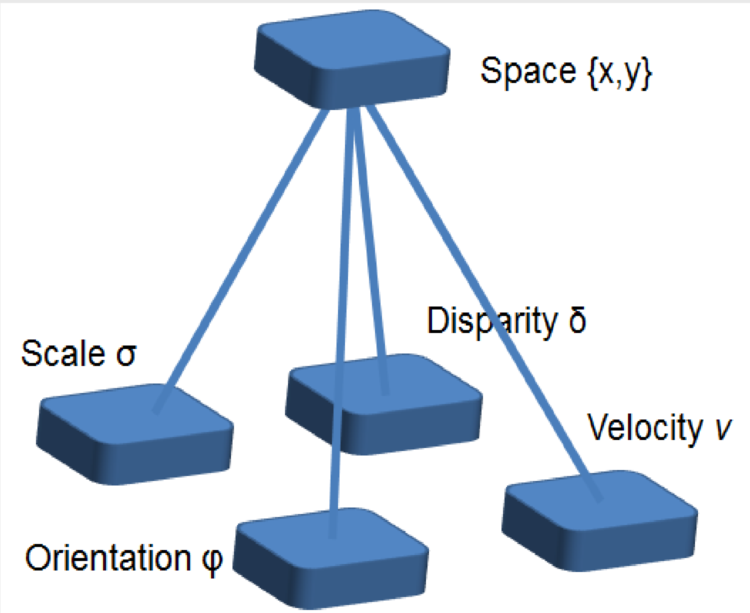

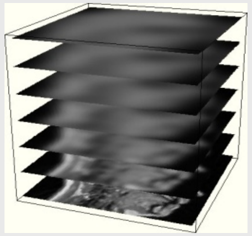

Multi-scale

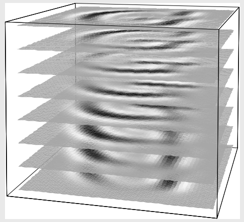

Multi-orientation

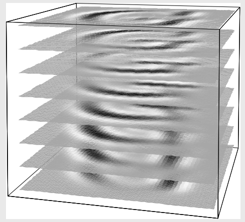

Multi-spatial frequency

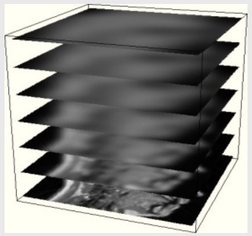

Multi-color

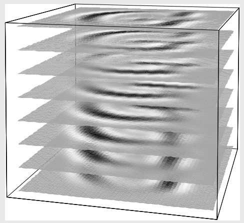

Multi-velocity

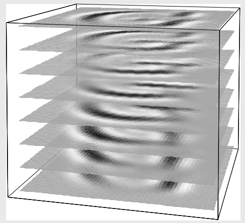

Multi-disparity

ERC grant Remco Duits, 2013-2018
EU project ‘MANET’

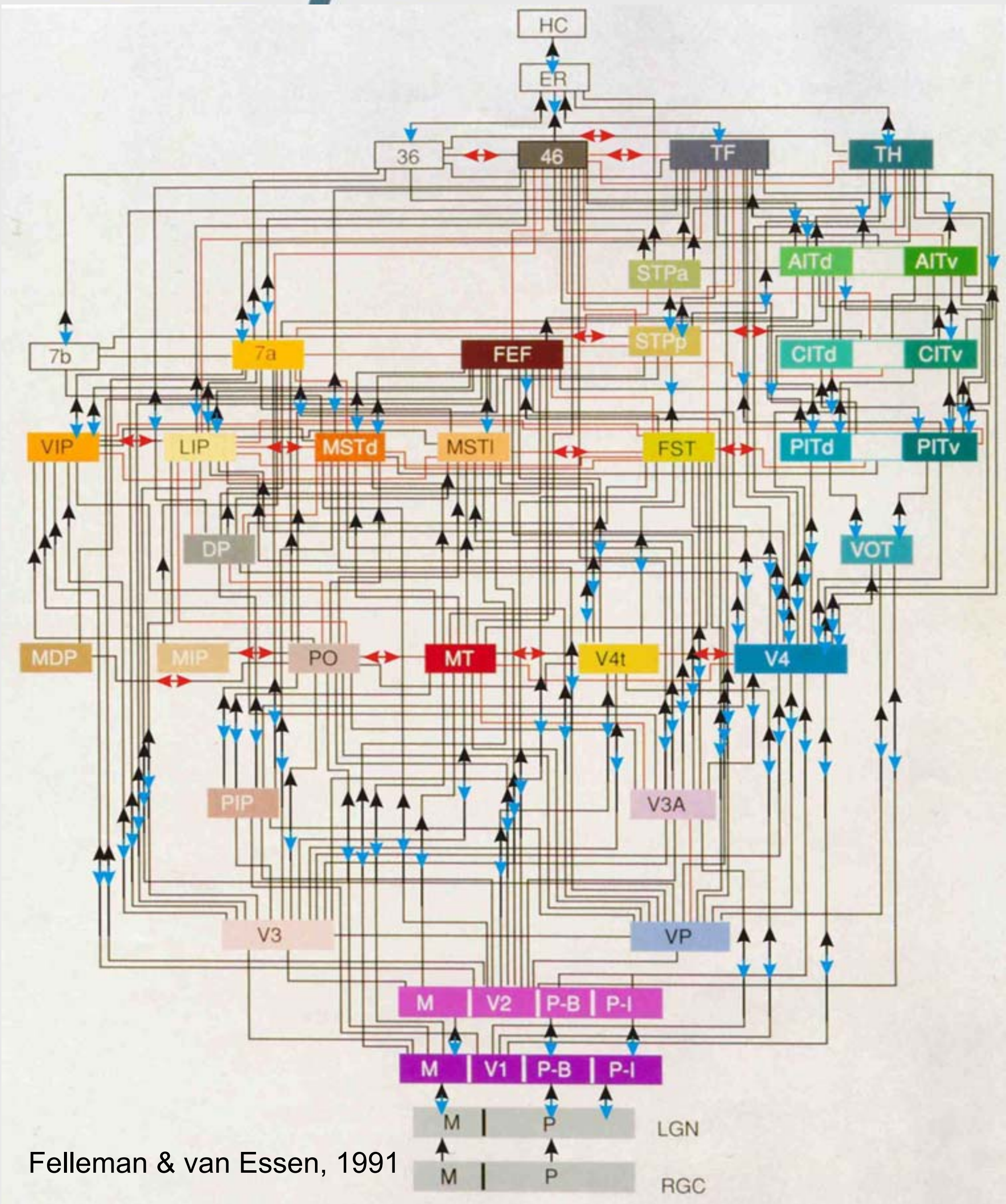

Felleman & van Essen, 1991

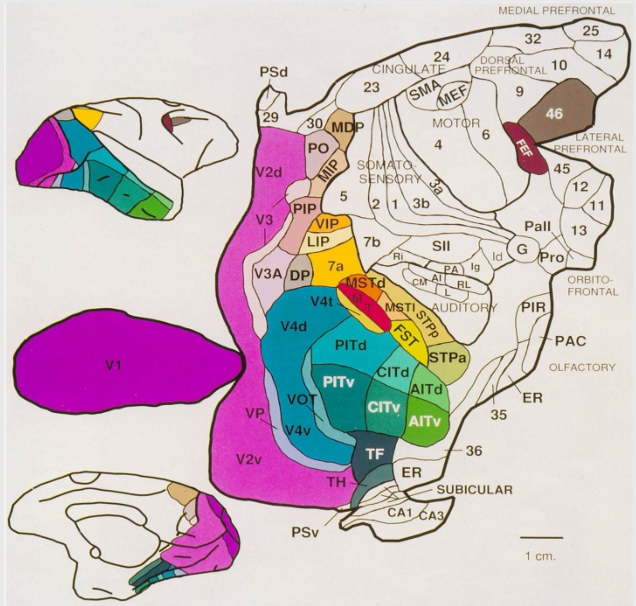

TU/e technische universiteit eindhoven

Math model for extensive filterbanks: Lie Group Vision

- Counter-intuitive: *add* dimensions
- Lie group theoretical model
- Axiomatic, first principles
  Context, Gestalt
- Massively parallel implementation

2D: 32 Mpixel, 6 scales, 64 orientations, 9 derivatives, 16 spatial frequencies, 3-64 colors, 16 velocities, 64 velocity directions, 16 disparities

3D: 1 Gvoxel, 6 scales, 64x32 orientations, 15 derivatives, 16 spatial frequencies, 3-64 colors, 16 velocities, 64x32 velocity directions

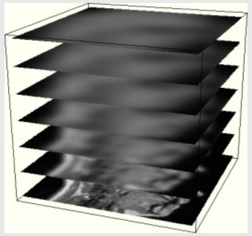

Multi-scale

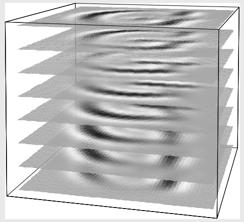

Multi-orientation

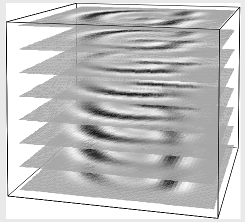

Multi-spatial frequency

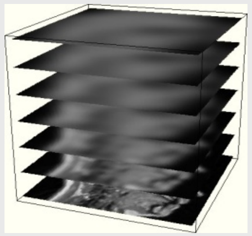

Multi-color

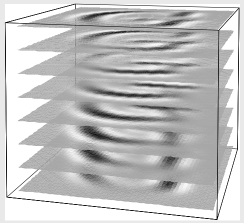

Multi-velocity

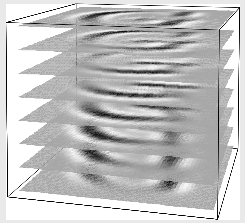

Multi-disparity

ERC grant Remco Duits, 2013-2018
EU project 'MANET'

technische universiteit eindhoven

Thanks!

Acknowledgements:

Remco Duits
Luc Florack
Anna Vilanova
Markus van Almsick
Erik Bekkers
Jiong Zhang
Erik Franken
Hans van Assen
Vesna Prckovska
Neda Sepasian
Mengmeng Tong
Marcel Breeuwer
Andrea Fuster
Tim Peeters
Stefan Meesters
Pauly Ossenblock
Bram Platel
Han van Triest
Paulo Rodriguez
Michiel Janssen
Fan Huang